



저작자표시-비영리-변경금지 2.0 대한민국

이용자는 아래의 조건을 따르는 경우에 한하여 자유롭게

- 이 저작물을 복제, 배포, 전송, 전시, 공연 및 방송할 수 있습니다.

다음과 같은 조건을 따라야 합니다:



저작자표시. 귀하는 원저작자를 표시하여야 합니다.



비영리. 귀하는 이 저작물을 영리 목적으로 이용할 수 없습니다.



변경금지. 귀하는 이 저작물을 개작, 변형 또는 가공할 수 없습니다.

- 귀하는, 이 저작물의 재이용이나 배포의 경우, 이 저작물에 적용된 이용허락조건을 명확하게 나타내어야 합니다.
- 저작권자로부터 별도의 허가를 받으면 이러한 조건들은 적용되지 않습니다.

저작권법에 따른 이용자의 권리는 위의 내용에 의하여 영향을 받지 않습니다.

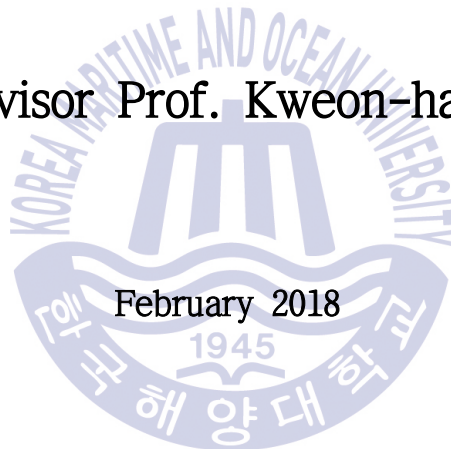
이것은 [이용허락규약\(Legal Code\)](#)을 이해하기 쉽게 요약한 것입니다.

[Disclaimer](#)

Master's Thesis

Investigation of the Effects of Baffles and Nozzles
on the Flow Characteristics in a Small Scrubber for
Marine Engines

Supervisor Prof. Kweon-ha Park



February 2018

Department of Mechanical Engineering
Graduate School of Korea Maritime and
Ocean University

Dai Xin

We certify that we have read this thesis and that, in our opinions, it is satisfactory in scope and quality as a thesis for the degree of Master of Mechanical Engineering, submitted by Dai Xin.

THESIS COMMITTEE

Chairperson: Prof. Ko, Ph.D.

Division of Mechanical Engineering
Korea Maritime and Ocean University

Co-Chairperson: Prof. Son, Ph.D.

Division of Mechanical Engineering
Korea Maritime and Ocean University

Supervisor: Prof. Park, Ph.D.

Division of Mechanical Engineering
Korea Maritime and Ocean University

February 2018

Department of Mechanical Engineering
Graduate School of Korea Maritime and Ocean University

Table of Contents

Table of Contents	iv
List of Tables	vi
List of Figures	vii
Abstract	xiii
Nomenclature	xv
Abbreviations	xvi
1. Introduction	1
1.1 Background	1
1.2 Performance of exhaust gas scrubber	4
1.3 Prospect of scrubber market	6
2. Investigation on the performance of baffles in a small scrubber	8
2.1 Calculation methods and conditions	8
2.1.1 Structure of scrubber	8
2.1.2 Calculation conditions	14
2.2 Analysis of scrubber with horizontal baffles	15
2.2.1 Analyzing baffle's length	15
2.2.2 Analyzing baffle's number	18
2.3 The optimal structure	22
2.4 Analysis of scrubber with vertical baffles	27
2.4.1 Analyzing baffle's length	27
2.4.2 Analyzing baffle's number	30

3. Investigation on the performance of sprays in a small scrubber	34
3.1 Mathematical models and conditions	34
3.1.1 Structure of scrubbers	34
3.1.2 Boundary conditions	38
3.2 Simulation and calculation results	39
3.2.1 Calculation conditions	39
3.2.2 Analyzing positions of nozzles	41
3.2.3 Analyzing numbers of nozzles	55
3.2.4 The optimal structure	65
4. Conclusion	77
Acknowledgement	79
References	81



List of Tables

Table 1 Specifications of vertical scrubber	9
Table 2 Specifications of horizontal scrubber	10
Table 3 Specification of exhaust gas	14
Table 4 Pressure drop of vertical scrubber with different length of baffles	15
Table 5 Length of streamline with different length ratios of baffles	17
Table 6 Pressure drop of vertical scrubber with different numbers of baffles	19
Table 7 Streamline distance of vertical scrubber with different numbers of baffles	20
Table 8 Pressure drop of horizontal scrubber with different lengths of baffles	27
Table 9 Streamline distance of horizontal scrubber with different length ratios of baffles	29
Table 10 Pressure drop of horizontal scrubber with different numbers of baffles	31
Table 11 Streamline distance of horizontal scrubber with different numbers of baffles	32
Table 12 Specifications of “D4AK-C” diesel engine	38
Table 13 Engine speed and gas flow rate	39
Table 14 Specifications of nozzles in research of nozzle location	40
Table 15 Specifications of nozzles in research of nozzle number	56
Table 16 Pressure drop of scrubber with different number of nozzles ..	60

List of Figures

Fig. 1 Map of emission control areas	1
Fig. 2 The evaluation of global sulphur legislation	3
Fig. 3 Emission reduction technology for marine diesel engines	5
Fig. 4 Sectional view of vertical scrubber	11
Fig. 5 Sectional view of horizontal scrubber	11
Fig. 6 3D-view of vertical scrubber with no baffle	12
Fig. 7 3D-view of vertical scrubber at two baffle	12
Fig. 8 3D-view of vertical scrubber at four baffle	12
Fig. 9 3D-view of vertical scrubber at six baffle	12
Fig. 10 3D-view of horizontal scrubber with no baffle	13
Fig. 11 3D-view of horizontal scrubber at two baffles	13
Fig. 12 3D-view of horizontal scrubber at four baffles	13
Fig. 13 3D-view of horizontal scrubber at six baffles	13
Fig. 14 Pressure drop of vertical scrubber with different length ratios of baffles	16
Fig. 15 Streamline distance of vertical scrubber with different length ratios of baffles	17
Fig. 16 Pressure drop of vertical scrubber with different numbers of baffles	19
Fig. 17 Streamline distance of vertical scrubber with different numbers of baffles	21
Fig. 18 Streamline distance of vertical scrubber at flow rate $70 [Nm^3/h]$	22
Fig. 19 Streamline distance of vertical scrubber at flow rate $100 [Nm^3/h]$	23

Fig. 20 Streamline distance of vertical scrubber at flow rate 130 [Nm^3/h]	23
Fig. 21 Streamline distance of vertical scrubber at flow rate 100 [Nm^3/h]	24
Fig. 22 Pressure contour of vertical scrubber at flow rate 70 [Nm^3/h]	24
Fig. 23 Pressure contour of vertical scrubber at flow rate 100 [Nm^3/h]	25
Fig. 24 Pressure contour of vertical scrubber at flow rate 130 [Nm^3/h]	25
Fig. 25 Pressure contour of vertical scrubber at flow rate 160 [Nm^3/h]	26
Fig. 26 Pressure drop of horizontal scrubber with different length ratios of baffles	28
Fig. 27 Streamline distance of horizontal scrubber with different length ratios of baffles	29
Fig. 28 Pressure drop of horizontal scrubber with different numbers of baffles	31
Fig. 29 Streamline distance of horizontal scrubber with different numbers of baffles	32
Fig. 30 Sectional view of vertical nozzles	36
Fig. 31 3D-view of vertical scrubber	37
Fig. 32 Mesh view of vertical scrubber	37
Fig. 33 Distribution of horizontal nozzles	40
Fig. 34 Distribution of vertical nozzles	41
Fig. 35 Pressure contour of vertical nozzles at flow rate 70 [Nm^3/h]	42

Fig. 36 Pressure contour of vertical nozzles at flow rate 100 [Nm^3/h]	42
Fig. 37 Pressure contour of vertical nozzles at flow rate 130 [Nm^3/h]	43
Fig. 38 Pressure contour of vertical nozzles at flow rate 160 [Nm^3/h]	43
Fig. 39 Pressure contour of horizontal nozzles at flow rate 70 [Nm^3/h]	44
Fig. 40 Pressure contour of horizontal nozzles at flow rate 100 [Nm^3/h]	44
Fig. 41 Pressure contour of horizontal nozzles at flow rate 130 [Nm^3/h]	45
Fig. 42 Pressure contour of horizontal nozzles at flow rate 160 [Nm^3/h]	45
Fig. 43 Comparison of pressure drop	46
Fig. 44 Comparison of streamline distance	46
Fig. 45 Streamline distance of vertical nozzles at flow rate 70 [Nm^3/h]	47
Fig. 46 Streamline distance of vertical nozzles at flow rate 100 [Nm^3/h]	47
Fig. 47 Streamline distance of vertical nozzles at flow rate 130 [Nm^3/h]	48
Fig. 48 Streamline distance of vertical nozzles at flow rate 160 [Nm^3/h]	48
Fig. 49 Streamline distance of horizontal nozzles at flow rate 70 [Nm^3/h]	49

Fig. 50 Streamline distance of horizontal nozzles at flow rate 100 [Nm^3/h]	49
Fig. 51 Streamline distance of horizontal nozzles at flow rate 130 [Nm^3/h]	50
Fig. 52 Streamline distance of horizontal nozzles at flow rate 160 [Nm^3/h]	50
Fig. 53 Water distribution of vertical nozzles at flow rate 70 [Nm^3/h]	51
Fig. 54 Water distribution of vertical nozzles at flow rate 100 [Nm^3/h]	52
Fig. 55 Water distribution of vertical nozzles at flow rate 130 [Nm^3/h]	52
Fig. 56 Water distribution of vertical nozzles at flow rate 160 [Nm^3/h]	53
Fig. 57 Water distribution of horizontal nozzles at flow rate 70 [Nm^3/h]	53
Fig. 58 Water distribution of horizontal nozzles at flow rate 100 [Nm^3/h]	54
Fig. 59 Water distribution of horizontal nozzles at flow rate 130 [Nm^3/h]	54
Fig. 60 Water distribution of horizontal nozzles at flow rate 160 [Nm^3/h]	55
Fig. 61 Distribution of two horizontal nozzles	56
Fig. 62 Distribution of three horizontal nozzles	57
Fig. 63 Distribution of four horizontal nozzles	57
Fig. 64 Distribution of five horizontal nozzles	58
Fig. 65 Distribution of six horizontal nozzles	58

Fig. 66 Distribution of seven horizontal nozzles	59
Fig. 67 Distribution of eight horizontal nozzles	59
Fig. 68 Streamline distance with different numbers of horizontal nozzles	61
Fig. 69 Streamline distribution of two horizontal nozzles at flow rate 160 [Nm^3/h]	61
Fig. 70 Streamline distribution of three horizontal nozzles at flow rate 160 [Nm^3/h]	62
Fig. 71 Streamline distribution of four horizontal nozzles at flow rate 160 [Nm^3/h]	62
Fig. 72 Streamline distribution of five horizontal nozzles at flow rate 160 [Nm^3/h]	63
Fig. 73 Streamline distribution of six horizontal nozzles at flow rate 160 [Nm^3/h]	63
Fig. 74 Streamline distribution of seven horizontal nozzles at flow rate 160 [Nm^3/h]	64
Fig. 75 Streamline distribution of eight horizontal nozzles at flow rate 160 [Nm^3/h]	64
Fig. 76 Water distribution of six horizontal nozzles at flow rate 70 [Nm^3/h]	65
Fig. 77 Water distribution of six horizontal nozzles at flow rate 100 [Nm^3/h]	66
Fig. 78 Water distribution of six horizontal nozzles at flow rate 130 [Nm^3/h]	66
Fig. 79 Water distribution of six horizontal nozzles at flow rate 160 [Nm^3/h]	67
Fig. 80 Temperature of six horizontal nozzles at flow rate 70 [Nm^3/h]	67

Fig. 81	Temperature of six horizontal nozzles at flow rate 100 [Nm^3/h]	68
Fig. 82	Temperature of six horizontal nozzles at flow rate 130 [Nm^3/h]	68
Fig. 83	Temperature of six horizontal nozzles at flow rate 160 [Nm^3/h]	69
Fig. 84	Streamline of six horizontal nozzles at flow rate 70 [Nm^3/h]	70
Fig. 85	Streamline of six horizontal nozzles at flow rate 100 [Nm^3/h]	70
Fig. 86	Streamline of six horizontal nozzles at flow rate 130 [Nm^3/h]	71
Fig. 87	Streamline of six horizontal nozzles at flow rate 160 [Nm^3/h]	71
Fig. 88	Pressure contour of six horizontal nozzles at flow rate 70 [Nm^3/h]	72
Fig. 89	Pressure contour of six horizontal nozzles at flow rate 100 [Nm^3/h]	73
Fig. 90	Pressure contour of six horizontal nozzles at flow rate 130 [Nm^3/h]	73
Fig. 91	Pressure contour of six horizontal nozzles at flow rate 160 [Nm^3/h]	74
Fig. 92	Vapor contour of six horizontal nozzles at flow rate 70 [Nm^3/h]	74
Fig. 93	Vapor contour of six horizontal nozzles at flow rate 100 [Nm^3/h]	75
Fig. 94	Vapor contour of six horizontal nozzles at flow rate 130 [Nm^3/h]	75
Fig. 95	Vapor contour of six horizontal nozzles at flow rate 160 [Nm^3/h]	76

Investigation of the Effects of Baffles and Nozzles on the Flow Characteristics in a small scrubber for Marine Engines

Dai Xin

Department of Mechanical Engineering
Graduate School of Korea Maritime and Ocean University

Abstract

A new version of “Rules for the Prevention of Air Pollution Caused by Ships” published by International Maritime Organization (IMO) on January 1, 2015. The regulation stipulated that the allowable emissions of sulphur oxides from ships in the Global Emission Control Area (ECA) was reduced from 1% to 0.1%, and the limitation on sulfur oxides in fuel oil used on board ships operating outside designated emission control areas will be reduced to 0.5%. Many technologies have been developed to meet the sulfur oxides limits by shipowners. Many types of devices are installed to reduce emission and to increase power efficiency, such as turbocharger, economizer, SCR, heat recovery system, catalytic converter, and scrubber etc. A turbocharger is a type of turbine-driven forced induction installation used to increase the power and efficiency of an internal combustion engine by intaking more air into the combustion chamber. SCR is a method for converting NO_x into N_2 and H_2O in the presence of a catalyst. An exhaust heat recovery system is a technology that translates thermal losses in the exhaust pipeline into energy to save fuel and reduce CO_2 emissions. Economizers are mechanical installations intended to reduce energy consumption or to preheat a fluid. A catalytic converter is a type of exhaust emission control device, and it is designed to convert toxic gases and pollutants into less toxic pollutants from the exhaust gas of an internal combustion engine by catalyzing a redox reaction.

Installing a marine exhaust gas scrubber is the best measure with the lowest cost and higher efficiency to convert NO_x into N_2 . Through a series of chemical and physical reactions, scrubber can clean up SO_x and particulates produced by diesel engines. Many researches have been put into different types of scrubbers. As one of the best measure, scrubber technologies have been developed and commercialized for low speed engines.

In this research, it was discussed that the influence of two different types of scrubber structures on pressure drop and flow streamlines. Pressure drop is a target related to the efficiency and power of diesel engine, and the flow streamlines is a target related to the duration for which the exhaust gas and cleaning water are in contact. It was also discussed the influence of the nozzle location and quantity on the cleaning water distribution. The length and number of horizontal and vertical baffles, and the number and location of nozzles were calculated and analyzed. The optimal inner structure was found out after fluid analysis of the scrubber for small marine engine, which shows that an inner structure with a baffle length ratio of 0.6 with two baffles was considered optimal in the case of a horizontal scrubber, and a baffle length ratio of 0.7 with two baffles was considered optimal in the case of a vertical scrubber. The result shows that the horizontal location is better than the vertical location, and the case of the six nozzles has the best performance in analyzing the influence of the nozzle location and quantity.

KEY WORDS: Scrubber, Baffle, Nozzle, Pressure drop, Streamline, Optimal structure

Nomenclature

IMO	International Maritime Organization
MARPOL	International Convention for the Prevention of Pollution from Ships
ECA	The Global Emission Control Area
LNG	Liquefied Natural Gas
DFDS	Det Forenede Dampskibs Selskab
SST	Shear stress transport
SO _x	Sulphur oxide
NO _x	Nitrogen oxide
rpm	Revolution per minute
ECC	European Economic Community
TEU	Twentyfoot equivalent unit
MGO	Marine gas oil
CFD	Computational fluid dynamics

Abbreviations

U	Velocity vector	m/s
γ	Stress	Pa
S_M	Momentum	kg.m/s
T	Temperature	°C
δ	Unit matrix	
ρ	Density	kg/m ³
p	Pressure	Pa
h	Enthalpy	kJ/kg
λ	Heat conduction ratio	W/m.K
v	Volume	m ³
u	Internal energy	J
S_E	The generated energy	J
k	Turbulence kinetic energy	m ² s ⁻²
ω	Specific dissipation rate	%
S	The strain rate magnitude	mm/min
a^*	Compensation factor	

Chapter 1 Introduction

1.1 Background

On January 1st, 2015, the International Maritime Organization (IMO) had officially implemented “The International Convention for the Prevention of Pollution From Ships” (MARPOL Annex VI). The conventional stipulation that the allowable emissions of sulphur oxides from ships in the Global Emission Control Area (ECA) will be reduced from 1% to 0.1%.



Fig. 1 Map of emission control areas

Fig. 1 shows the area of ECA in the world [1]. So far, Denmark, Finland, the Netherlands, Sweden and Norway which are the countries in ECA had announced they would increase the SO_x emissions monitoring and penalties soon. Denmark would detect SO_x emissions from ships in the air through unmanned aerial vehicle sniffing technology and the installation of fixed

sniffer devices under the bridge to detect whether sulphur content has dropped from 1% to 0.1%, and would use the latest portable onboard measurement tools to increase the frequency of fuel sample collection and monitoring. The similar measurement were introduced in Finland, the Netherlands and other countries.

This regulation forces ship operators to use all necessary measures to reduce sulphur oxide emissions. Marine fuels emit sulfur oxides, nitrogen oxides and particulates into the atmosphere during combustion, which will pollute the ecosystem. In 2011, according to the “MARPOL Annex VI” approved by IMO. It allowed ship operators to reduce pollutant emissions by changing fuel specifications, types, or using exhaust gas scrubbers. The agreement not only stipulated the limit maximum emissions of pollutants worldwide, but also imposed stricter standards on designated sea areas. According to Fig. 2, since 2015, in North America, the Baltic Sea, the North Sea and the Caribbean Sea, the upper limit of sulphur oxide emissions for marine vessels has been reduced from 1% to 0.1%. In all European waters except ECA, the upper limitation sulphur oxide emissions from ships will be reduced by 0.5% and further reduce to 0.1% by 2020, and the new criterion of 0.5% sulphur oxide emissions by 2020 or 2025 will come into effect globally. For most new ships, installing exhaust gas scrubbers would save a lot of money if they planned to sail for longer periods of time at ECA. A 1100 TEU container ship fitted with an exhaust gas scrubber will be refunded for three years if it has been operating within the ECA.

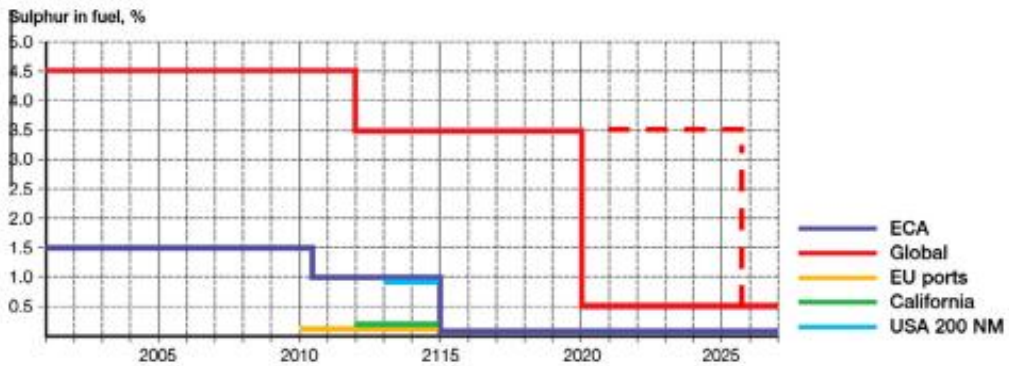


Fig. 2 The evaluation of global sulphur legislation

In order to reduce the sulfur oxide content in ship exhaust gas, many ship operators had taken action. Nowadays, there are three main measures to control the emission of sulfur oxides from ships. One is to use low sulfur oil, the other is to replace dual fuel engine for ships, and the third is to install exhaust gas scrubber. The use of low sulfur oil could also increase the cost of shipping operators, given that crude oil prices could rise sharply in the future. The installation of marine exhaust gas scrubber is the most economical and effective scheme in addition to the use of low sulfur oil. Exhaust gas scrubber can use seawater or fresh water to clean ship exhaust gas. The sulfur oxide is basically removed from the exhaust gas as well. This technology allows ship operators to continue using heavy oil instead of expensive light diesel. Solvang which is a ship company in Norway installed exhaust scrubbers for two liquefied natural gas (LNG) ships built by Hyundai Heavy Industries. Det Forenede Dampskibs Selskab (DFDS) which is a shipbuilder in Danmark installed exhaust scrubbers on twenty-one ships at a cost of about 140 million dollars in 2017. Carnival, which is a leading luxury cruise operator, announced in 2016 that it would invest 400 million dollars to install exhaust scrubber for seventy cruise ships. With the expansion and increase of ECA in the world and the imposing requirements for

environmental protection, the orders of many scrubber companies for ship scrubbers have increased dramatically. The market of ship exhaust gas scrubber may be entering a golden period of development. Wachelan recently announced that it had received an order for a total of ninety-four exhaust gas scrubber units for forty-five ships, involving new shipbuilding and conversion projects. Afalavat had recently signed a contract with Seif, the largest shipping company in the Netherlands, and to provide it with the world's largest marine exhaust gas scrubbers.

1.2 Performance of exhaust gas scrubber

There are many technologies to reduce emissions, which are shown in Fig. 3. Installing an exhaust gas scrubber has high cost performance by comparing with other methods. The “MARPOL Annex” makes the market of ship exhaust gas scrubber flourish. However, some experts still questioned the installation of large and expensive scrubber equipment on the ship. The chief executive officer of Maersk Line, which is a shipping company, said in public that it might not make much sense to install such expensive and large equipment for container ships. He said that there were a number of reasons for his questioning, including the large area occupied by the exhaust scrubber, which was not cost-effective for container ships with high requirements for the utilization of cabin capacity. When a scrubber separates sulphur from the exhaust gas, the disposal of residue will also produce certain expenses and so on. These will significantly increase the cost of ship operators.

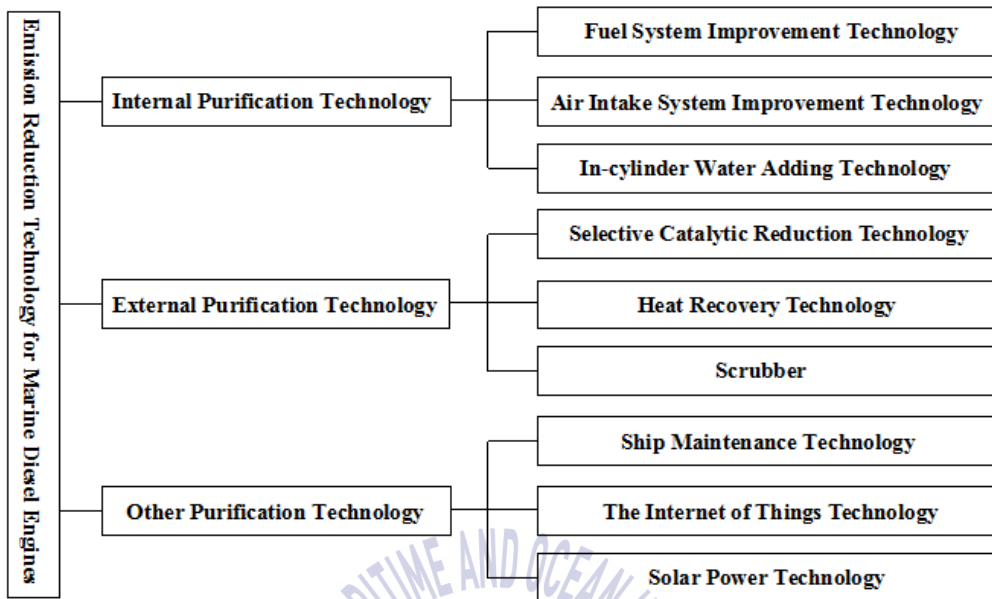


Fig. 3 Emission reduction technology for marine diesel engines

The experts said it is better to install a exhaust gas scrubber in tankship than container. The space of container ship is limited. It is not suitable to install large scrubber, and the cost of refit is very high. By contrast, the tankship has much more room to install equipment. At the same time, the size of the ship is also the factor of installing exhaust scrubber. It is cheaper to install scrubbers on large ships. More factors need to be analyzed when install exhaust gas scrubber to operational ships than new ships. Types of ship, size, design and structure of ships should also be taken into account. In addition, the use time of ECA and the annual fuel consumption of ships should be considered in the selection of exhaust gas scrubber. To deal with the residue after washing, the EEC Shipowner Association recently called for further clarification of ship exhaust gas scrubber regulations. The association said the scrubber used seawater to remove sulfur oxides from ships and then

released sea water back into the sea, which could still cause damage to the environment. Therefore, the approval process of the product should be adjusted and reflected in IMO conventions. It is the regulatory uncertainty and possible processing costs that make Maersk Line, the European Container Company and other companies less motivated to install exhaust gas scrubbers or delay plans to install them.

However, installing an exhaust gas scrubber is a better choice in terms of cost and effectiveness, compared with other ways to control the sulphur oxide emissions in ships. Besides installing exhaust scrubber, ship operators can reduce sulfur oxide emissions by using light diesel or liquefied natural gas (LNG). At present, the price of conventional fuel used in navigation is about 650 dollars per ton, while the price of light diesel oil is 1050 dollars per ton. There is an evidence that the cost of cargo transportation will rise by nearly 30% by using a marine light diesel alternative to the Baltic spur line, and that the long-term use of low sulphur diesel may also cause damage to equipment such as engines. While it is technically feasible for ships to use LNG, the cost of construction or alteration is high. At the same time, the addition of LNG storage tanks will reduce the cargo loading space, and supply facilities are immature. These will greatly increase the cost of operators. The research showed that some of the exhaust gas scrubbers have experience of working for ten thousands of hours, and the effect of sulfur oxide removal is obvious. The device pumps water or fresh water or chemicals into the sea to remove sulphur oxide from turbine exhaust gas, as well as most of soot and particulate matter. Therefore, the installation of ship scrubber is still a relatively high cost performance program.

1.3 Prospect of scrubber market

There had been 30% or 40% of new ships installed with exhaust gas scrubber till 2016, which created a market of 10 billion euros. As shown in Fig. 2, the new rule on sulphur oxide emission of 0.5% by 2020 or 2025 will come into effect globally, even approach to 0.1% in some EU ports and America except ECA [1][2]. All strict rules will make the market of ship exhaust gas scrubber expand dramatically further. This huge market promotes the rapid development of ship scrubber technology, and many ship companies spare no effort in developing products, passing classification society certification, competing for orders, purchasing enterprises for resource integration, and so on. For example, GTM in Greece, Langh Shipping in Finland and other companies have passed classification society certification for their exhaust gas scrubbers, while Yala International Company is acquiring a 63% stake in GTM, expanding its business scale in ECA. With the promotion and implementation of the “SO_x Limitation Convention”, the market of exhaust gas scrubber will be flourish.

Chapter 2 Investigation on the performance of baffles in a small scrubber

2.1 Calculation methods and conditions

2.1.1 Structure of scrubber

Many equipments are installed in an internal combustion engine to reduce emissions and increase thermal efficiency. A turbocharger is a type of turbine-driven forced induction installation used to increase the power and thermal efficiency of an internal combustion engine by intaking more air into the combustion chamber [3]–[5]. SCR is a method for converting NO_x into N_2 and H_2O in the presence of a catalyst. It is widely used in diesel engines to reduce NO_x . Kuroki et al. studied a type of commercial-scale indirect plasma and chemical hybrid system that was fifteen times more economical than the conventional SCR system [6]. An exhaust heat recovery system is a technology that translates thermal losses in the exhaust pipeline into energy to save fuel and reduce CO_2 emissions. Kyriakidis et al. optimized a model of a waste heat recovery system for a two-stroke marine diesel engine [7]. Economizers are mechanical installations intended to reduce energy consumption or to preheat a fluid [8]. Acatalytic converter is a type of exhaust emission control device, and it is designed to convert toxic gases and pollutants into less toxic pollutants from the exhaust gas of an internal combustion engine by catalyzing a redox reaction [9]. A scrubber is an important installation in an internal combustion engine for reducing SO_x emissions. Many studies on scrubbers have been conducted [10]–[13]. Bal et al. studied the fluid flow behavior and the effect of different parameters on pressure drop in a Venturi scrubber [8]. In this research, it is concerned with the influence of two

different types of scrubber structures on pressure drop and streamlines. Pressure drop is closely related to the power and efficiency of the engine, and the behavior of the flow streamlines is related to the duration for which the exhaust gas and cleaning water are in contact [14]-[17]. By using ANSYS to simulate the scrubber with horizontal and vertical baffles, respectively. The testing variables are the length, number, and the distance of baffles. According to the data of two groups of model, the optimal structure was discovered. under exhaust gas of 1000 Pa.

This simulation was based on the actual size of marine scrubber tower and the working speed of diesel engine. The model was modeled by NX9.0 and use ANSYS CFX to do the fluent calculation. We found out the relation between pressure drop, streamline distance and the length of baffles, the number of baffles under four different velocities of exhaust gas. Two types of scrubber models were used in this simulation. Both volumes were 60 L. We calculated the velocities of ideal exhaust gas are 7.44 m/s, 10.62 m/s, 13.8 m/s, and 16.98 m/s according to the flow rate generated by D4AK-C diesel engine. The diameter of inlet and outlet pipes are 100mm. Horizontal scrubber is 1000mm in length, 300mm in width and 200mm in height. Vertical scrubber is 400mm in length, 200mm in width and 750mm in height. The testing variables are the baffle length and number. The specification of two scrubbers are shown in Table 1, and Table 2.

Table 1 Specifications of vertical scrubber

Number of baffle	0	2	4	6	
Length of scrubber L_1 [mm]	400				
Length of baffle l_1 [mm]	l_1/L_1	0.5	0.6	0.7	0.8
	l_1 [mm]	200	240	280	3200
Gap between baffles [mm]	92				

Table 2 Specifications of horizontal scrubber

Number of baffle	0	2	4	6	
Length of scrubber L_2 [mm]	1000				
Length of baffle l_2 [mm]	l_2/L_2	0.5	0.6	0.7	0.8
	l_2 [mm]	500	600	700	800
Gap between baffles [mm]	100				

Two types of scrubbers were used in the calculation. The volumes were 60 L. The two-dimensional and three-dimensional patterns were set up by NX 9.0. The sectional views are shown in Fig. 4 and Fig. 5. The three-dimensional views of horizontal scrubbers are shown in Fig. 6-Fig. 9, and the three-dimensional views of vertical scrubbers are shown in Fig. 10-Fig. 13.

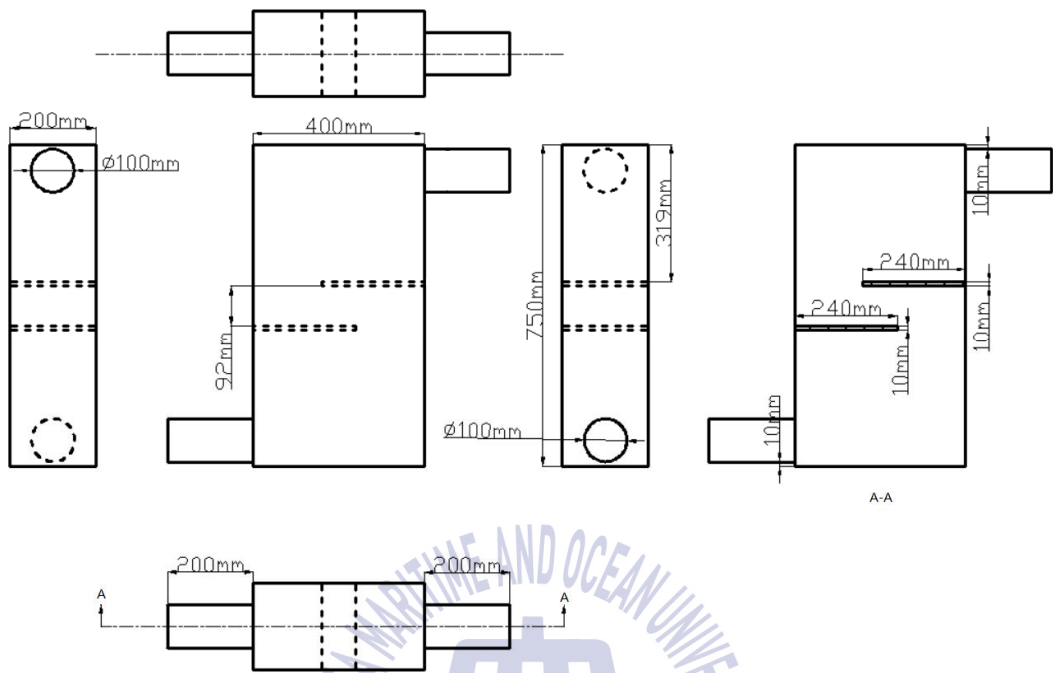


Fig. 4 Sectional view of vertical scrubber

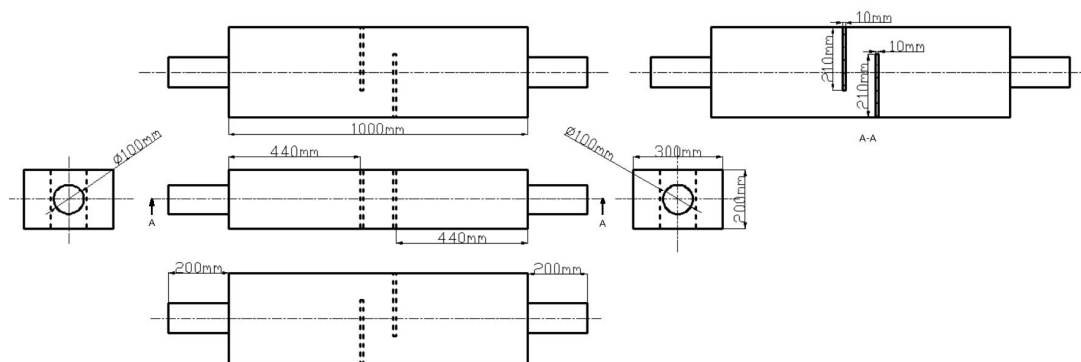


Fig. 5 Sectional view of horizontal scrubber

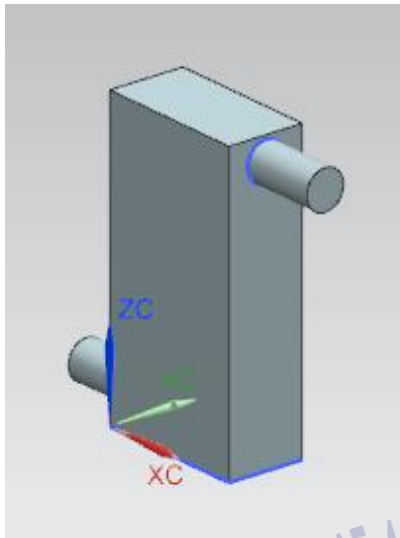


Fig. 6 3D-view of vertical scrubber with no baffle

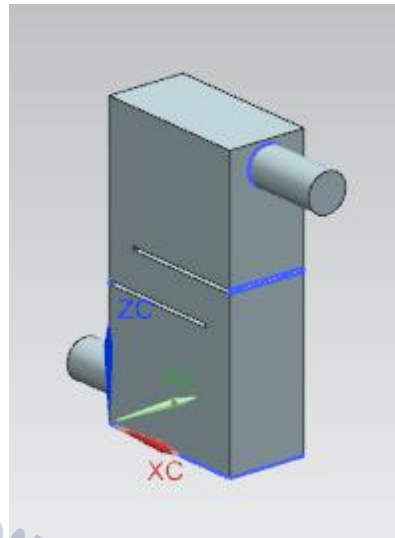


Fig. 7 3D-view of vertical scrubber at two baffles

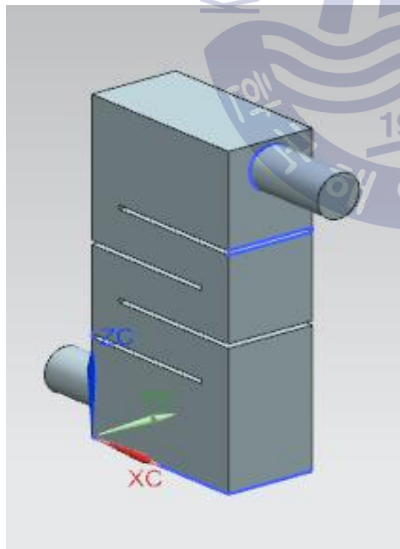


Fig. 8 3D-view of vertical scrubber at four baffles

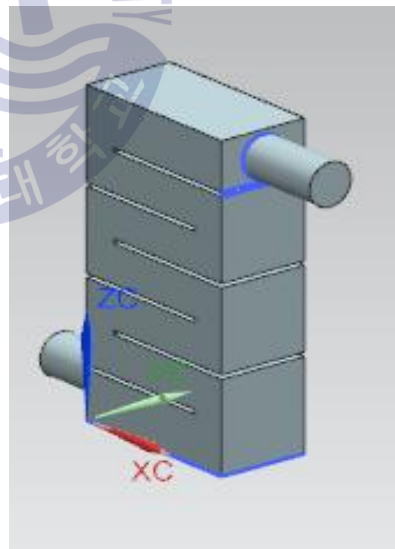


Fig. 9 3D-view of vertical scrubber at six baffles



Fig. 10 3D-view of horizontal scrubber with no baffle

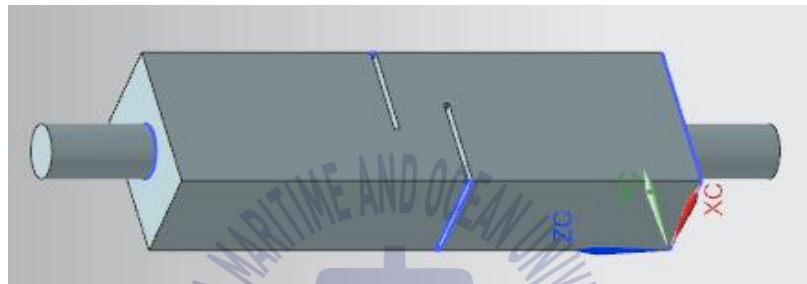


Fig. 11 3D-view of horizontal scrubber at two baffles

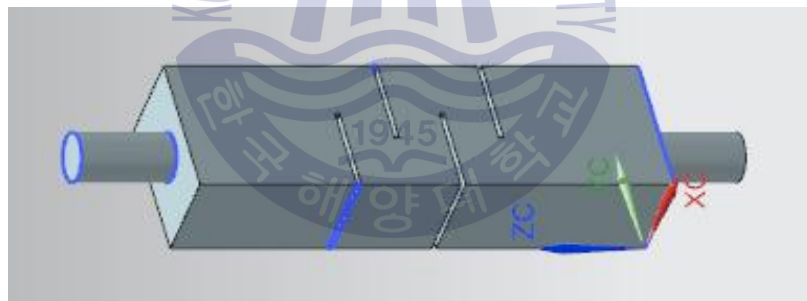


Fig. 12 3D-view of horizontal scrubber at four baffles

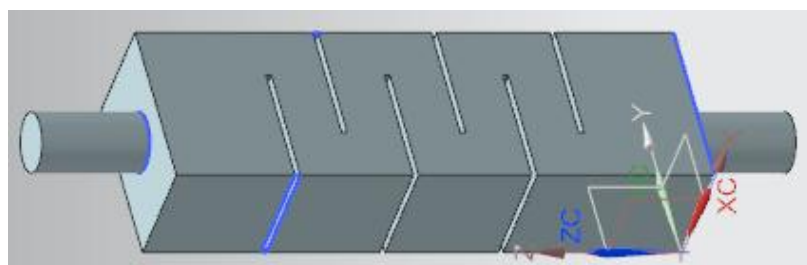


Fig. 13 3D-view of horizontal scrubber at six baffles

2.1.2 Calculation conditions

The test was simulated under four different flow rate generated by a diesel engine D4AK-C. This simulation considered the gravity. Here are the mathematical formulas, and the specifications of flow rate and velocities of exhaust gas are shown in Table 3.

Table 3 Specifications of exhaust gas

Engine speed [rpm]	Flow rate [Nm^3/h]	Velocity [m/s]
700	70	7.44
1000	100	10.62
1300	130	13.8
1600	160	16.98

Continuous Equation

$$\frac{\partial \rho}{\partial t} + \nabla \cdot (\rho U) = 0 \quad (1)$$

Momentum Equation

$$\frac{\partial(\rho U)}{\partial t} + \nabla \cdot (\rho U \otimes U) = -\nabla p + \nabla \cdot r + S_M \quad (2)$$

$$r = \mu(\nabla U + (\nabla U)^T) - \frac{2}{3}\delta \nabla \cdot U \quad (3)$$

Energy Equation

$$\frac{\partial(\rho h)}{\partial t} + \nabla \cdot (\rho U h) = \nabla \cdot (\lambda \nabla T) + \gamma : \nabla U + S_E \quad (4)$$

$$h = u + pv \quad (5)$$

U is velocity vector, γ is stress, S_M is momentum, T is temperature, δ is a

unit matrix, ρ is density, p is pressure, h is enthalpy, λ is heat conduction ratio, v is volume, u is internal energy and S_E is the generated energy. SST (Shear Stress Transport) model is used to calculate turbulent flow.

The Turbulent Viscosity

$$\mu_t = \frac{\rho k}{w} \frac{1}{\max\left[\frac{1}{a^*}, \frac{SF_2}{a_1 w}\right]} \quad (6)$$

The Blending Function

$$\theta_2 = \max\left(2 \frac{\sqrt{k}}{0.09 \omega y}, \frac{500 v}{\rho y^2 \omega}\right) \quad (7)$$

$$F_2 = \tanh(\theta_2^2) \quad (8)$$

k is turbulence kinetic energy, ω is specific dissipation rate, ρ is density, S is the strain rate magnitude, a^* is compensation factor.

2.2 Analysis of scrubber with horizontal baffles

2.2.1 Analyzing baffle's lengths

After simulating scrubbers with two different length of baffles and empty one respectively. The simulation results are shown in Table 4, and Fig. 14.

Table 4 Pressure drop of vertical scrubber with different length of baffles

Item [Nm^3/h]	Empty [Pa]	Ratio0.5 [Pa]	Ratio0.6 [Pa]	Ratio0.7 [Pa]	Ratio0.8 [Pa]
Flow Rate-70	129	128	128	138	155
Flow Rate-100	259	254	257	276	321
Flow Rate-130	427	424	422	459	512
Flow Rate-160	637	629	625	679	760

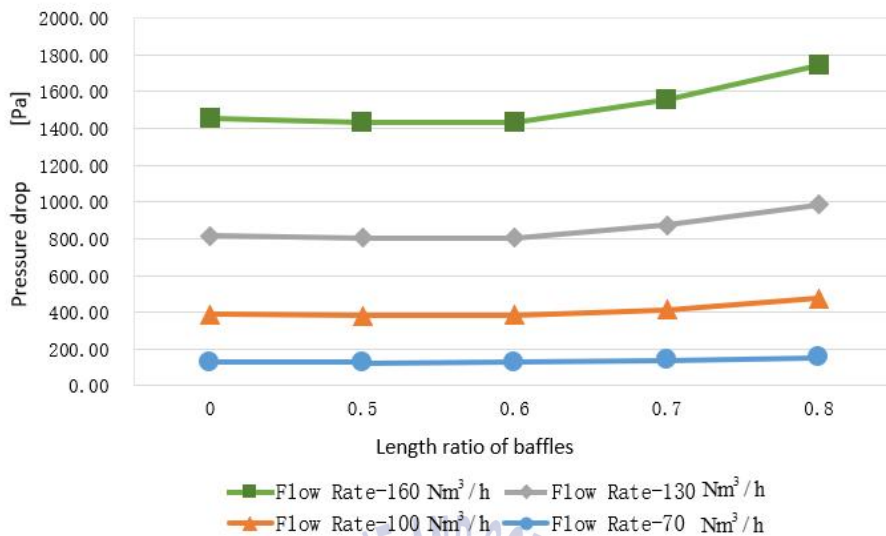


Fig. 14 Pressure drop of vertical scrubber with different length ratios of baffles

According to Fig. 14, with the increase of gas flow rate, the pressure drop increased with the increase of baffle length. At a flow rate of $70 \text{ Nm}^3/\text{h}$, with the increase of baffle length from 0 to ratio 0.8, There was no obvious change in pressure drop, which remained at 130Pa. At a flow rate of $100 \text{ Nm}^3/\text{h}$, the pressure drop of empty scrubber is 259Pa, and Pressure drop of scrubber with length ratio of 0.5 is 254Pa. Ratio 0.6 one is 257Pa. It indicated that with increase of baffle lengths, there was no obvious change in pressure drop. However, when the baffle length increased from ratio 0.7 to 0.8, the pressure drop increased from 276Pa and 321Pa as well. It indicated that the pressure drop had a low increase level with the increase of baffle length. At a flow rate of $130 \text{ Nm}^3/\text{h}$, with the increase of baffle length, The pressure drop of empty scrubbers, scrubber in ratio 0.5, and scrubber in ratio 0.6 had no significant change and maintained at about 425Pa. From ratio 0.6 to ratio 0.8, Pressure drop emerged an increasing trend. At a flow rate of $160 \text{ Nm}^3/\text{h}$,

the increase trend of pressure drop is same as in $130Nm^3/h$. There was no big difference from empty to ratio 0.6. The increase level was high from length ratio of 0.6 to 0.8. It could conclude that the baffle length should be less than ratio 0.6 when designing the small horizontal scrubber. After simulation by ANSYS, the streamline distance of scrubber with horizontal baffles are shown in Table 5, and Fig. 15.

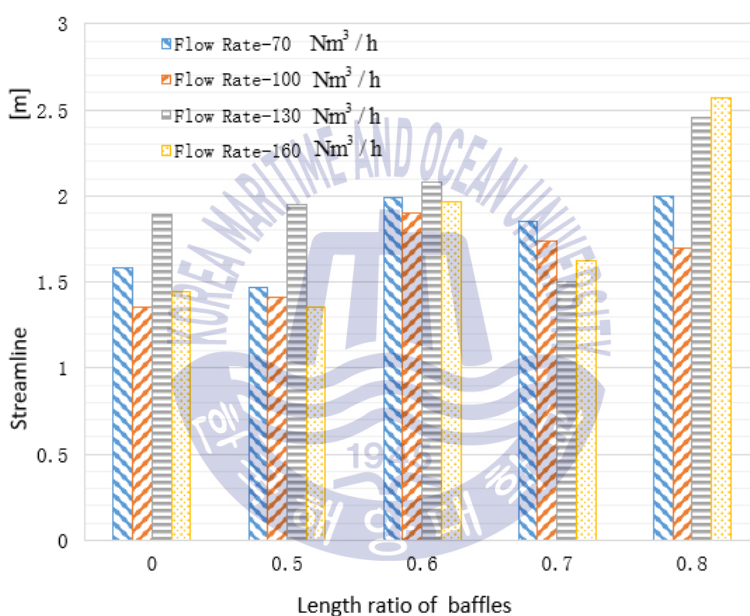


Fig. 15 Streamline distance of vertical scrubber with different length ratios of baffles

Table 5 Length of streamline with different length ratios of baffles

Item [Nm^3/h]	Empty [m]	Ratio0.5 [m]	Ratio0.6 [m]	Ratio0.7 [m]	Ratio0.8 [m]
Flow Rate-70	1.58	1.47	1.99	1.85	2
Flow Rate-100	1.11	1.41	1.9	1.74	1.7
Flow Rate-130	1.89	1.95	2.08	1.50	2.46
Flow Rate-160	1.44	1.35	1.97	1.62	2.57

Streamline distance indicates the mixing time of exhaust gas and cleaning water. The longer streamline distance is, the longer mixing time is. According to Fig. 15, at a flow rate of $70Nm^3/h$, The streamline distance of ratio 0.8 and ratio 0.6 were the largest and the second large. They were 2m and 1.99 m long, respectively. The minimum streamline distance was ratio 0.5, which was 1.47m. At a flow rate of $100Nm^3/h$, the maximum streamline distance was length ratio 0.6, which was 1.9m. The minimum streamline distance was 1.11 m at empty scrubber. At a flow rate of $130Nm^3/h$, The maximum streamline distance was 2.46m at ratio 0.8. The minimum streamline distance was at ratio 0.7, which was 1.26m. When the flow rate is $160Nm^3/h$, the maximum streamline distance was 2.57m at ratio 0.8. Ratio 0.6 was the second large, and the minimum streamline distance was at ratio 0.5, which was 1.35 m. After analysing streamline distance of four scrubbers under four different flow rates, it indicated that the difference of streamline distance among ratio 0.6 were smaller, which meant they were more steady. Secondly, the streamline distances at ratio 0.6 were longer than other cases, only shorter than ratio 0.8. It indicated that at ratio 0.6, there was more time to mix the exhaust gas with washing liquid. It could concluded that the baffle length at ratio 0.6 were the optimal scheme when designing this small vertical scrubber for marine engines, in conjunction with the pressure drop and the streamline distance distribution.

2.2.2 Analysing baffle's numbers

The above simulation proved that scrubber at ratio 0.6 was the optimal structure. The horizontal scrubber at baffle length ratio 0.6 was selected in this simulation. The variable was the baffle number, which was divided into four groups. The number of baffles in each group were 0, 2, 4 and 6, respectively. The pressure drop of horizontal scrubber with different numbers

of baffle are shown in Table 6, and Fig. 16 after simulating by ANSYS.

Table 6 Pressure drop of vertical scrubber with different numbers of baffles

Item [Nm^3/h]	Empty [Pa]	2-Baffles [Pa]	4-Baffles [Pa]	6-Baffles [Pa]
Flow Rate- 70	129	128	167	284
Flow Rate-100	259	257	336	567
Flow Rate-130	427	422	559	960
Flow Rate-160	637	625	835	1470

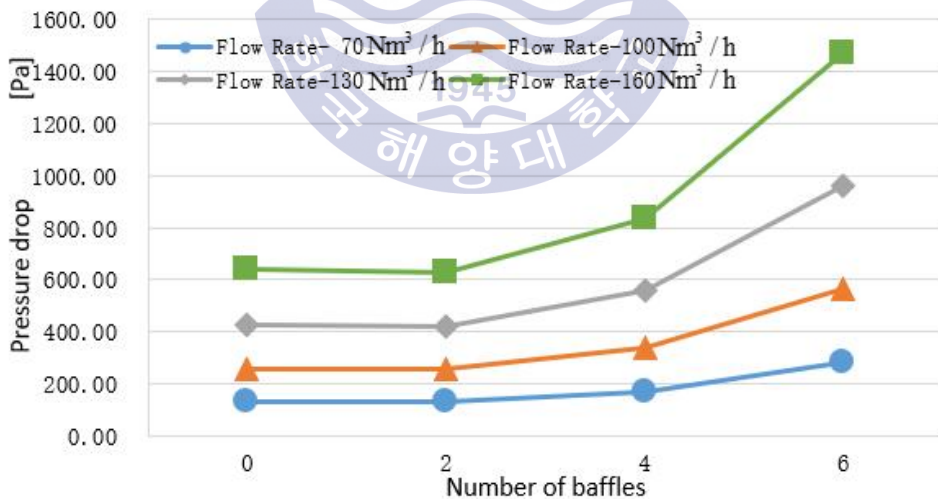


Fig. 16 Pressure drop of vertical scrubber with different numbers of baffles

According to Table 6 and Fig. 16, at a flow rate of $70Nm^3/h$, when the baffle number increased from 0 to 2. Pressure drop had no obvious change. the former was 129Pa, and the latter was 128Pa. When the number of baffles increased from 2 to 6, pressure drop increased from 128Pa to 284Pa. At a flow rate of $100Nm^3/h$, there was no change of pressure drop when the number of baffles increased from 0 to 2. When the number of baffles increased from 2 to 6, pressure drop increased from 257Pa to 567Pa. At a flow rate of $130Nm^3/h$, with the number increased from 0 to 2, there was no big change of pressure drop. The pressure drop increased from 422Pa to 960 Pa with the baffle number increased from 2 to 6. At a flow rate of $160 Nm^3/h$, there was no big change of pressure drop when the baffle number increased from 0 to 2. The increase level was very obvious with baffle number increased from 2 to 6, and pressure drop increased from 625Pa to 1470Pa. The result showed that with the increase of baffle number from 0 to 2, pressure drop kept no obvious change under four different flow rates. The pressure drop increases at a high level with the baffle number increased from 2 to 6. The number of baffles should be less than 2 when designing this type of scrubber. After simulating by ANSYS, the streamline distances are shown in Table 7, and Fig. 17.

Table 7 Streamline distance of vertical scrubber with different numbers of baffles

Item [Nm^3/h]	Empty [m]	No.2 [m]	No.4 [m]	No.6 [m]
Flow Rate- 70	1.58	1.99	2.1	1.87
Flow Rate-100	1.35	1.9	2.1	1.24
Flow Rate-130	1.89	2.08	1.61	1.67
Flow Rate-160	1.44	1.97	1.83	1.58

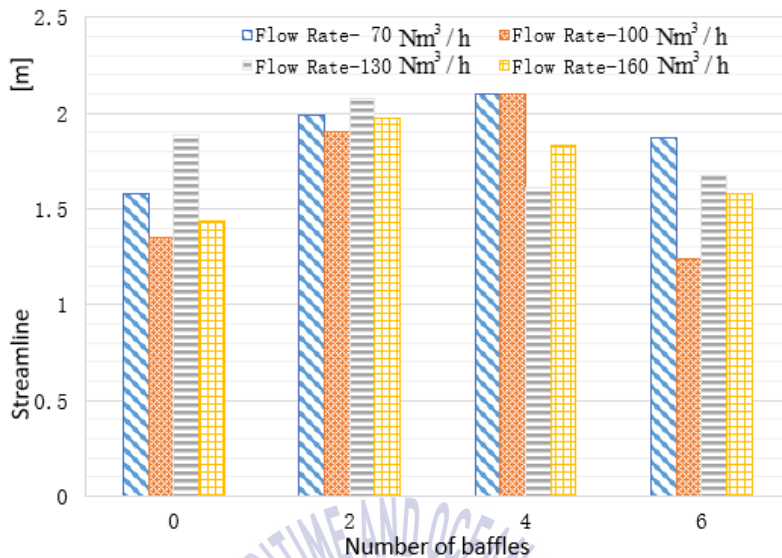


Fig. 17 Streamline distance of vertical scrubber with different numbers of baffles

From Fig. 17 and Table 7, at a flow rate of $70Nm^3/h$, streamline distance of scrubber with 4 baffles was the longest, which was 2.1m. The second one was 2 baffles, which was 1.99m. The streamline distance of empty scrubber was the shortest, which was 1.58m. At a flow rate of $100Nm^3/h$, the streamline distance of scrubber with 4 baffles was the longest, which was 2.1 m. 2 baffles was the second. Scrubber with 6 baffles was the shortest, which was 1.24m. At a flow rate of $130Nm^3/h$, the streamline distance of scrubber with 2 baffles was the largest, which was 2.08m. Streamline of scrubber with 4 baffles was the smallest, which was 1.61m. When the flow rate is $160 Nm^3/h$, the longest streamline distance was 2 baffles, which is 1.97m. The empty scrubber was the smallest one, which was 1.44m. According to Fig. 18, the streamline distance at 2 baffles were the longest under different flow rates, which indicated it had the longest distance to mix exhaust gas and

cleaning water. Scrubber with 4 baffles are also in good performance. When designing this type of scrubber, baffle numbers should be designed in 2 or 4.

In conclusion, combining with the distributions of pressure drop and streamline distance, the optimal structure is 2 baffles and length ratio of 0.6.

2.3 The optimal structure

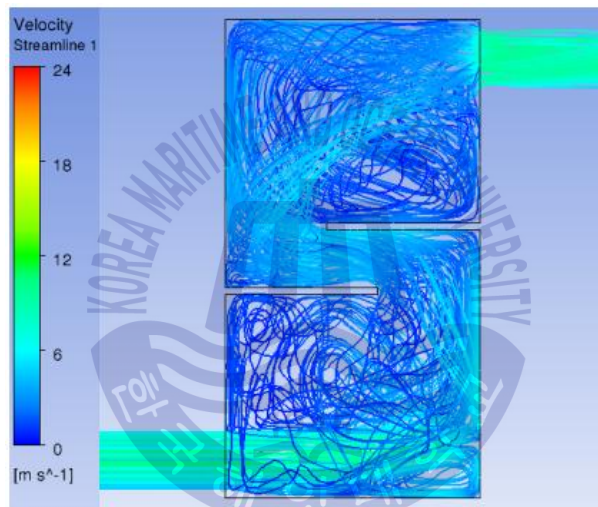


Fig. 18 Streamline distance of vertical scrubber at flow rate $70 [Nm^3/h]$

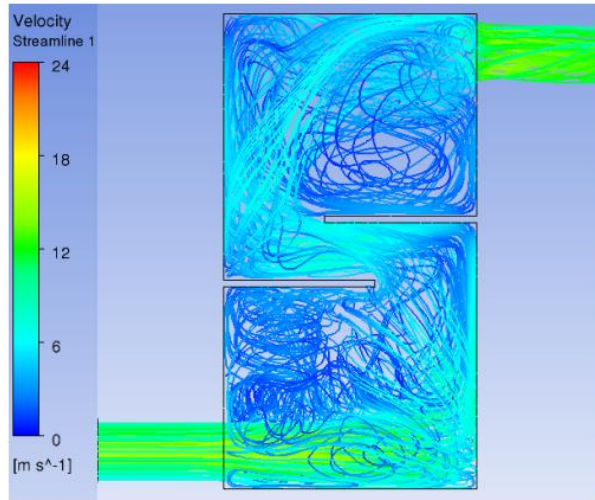


Fig. 19 Streamline distance of vertical scrubber at flow rate 100 [Nm^3/h]

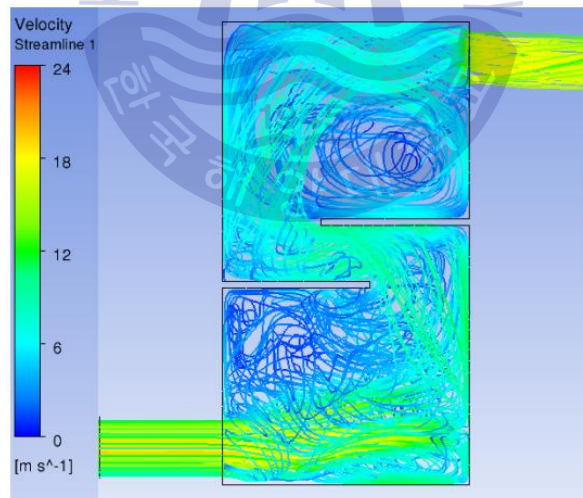


Fig. 20 Streamline distance of vertical scrubber at flow rate 130 [Nm^3/h]

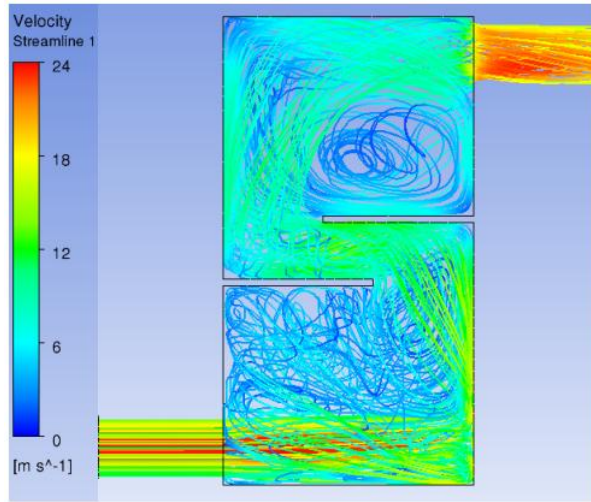


Fig. 21 Streamline distance of vertical scrubber at flow rate 160 [Nm^3/h]

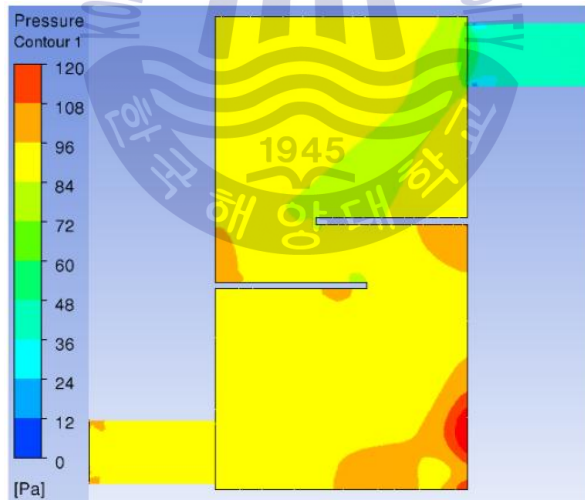


Fig. 22 Pressure contour of vertical scrubber at flow rate 70 [Nm^3/h]

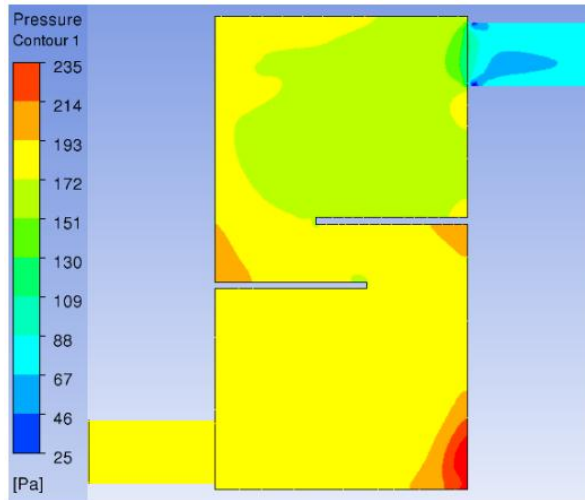


Fig. 23 Pressure contour of vertical scrubber at flow rate 100 [Nm^3/h]

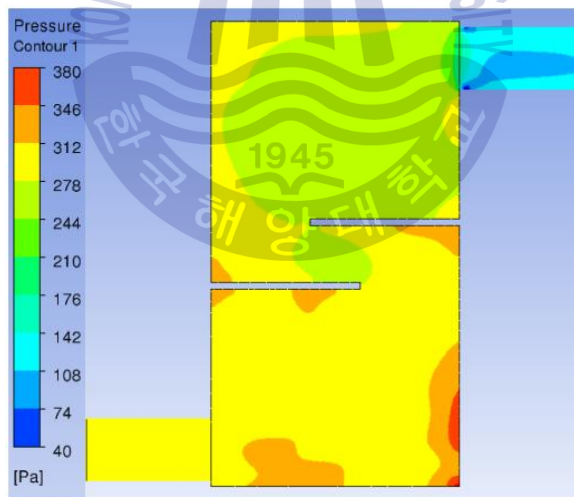


Fig. 24 Pressure contour of vertical scrubber at flow rate 130 [Nm^3/h]

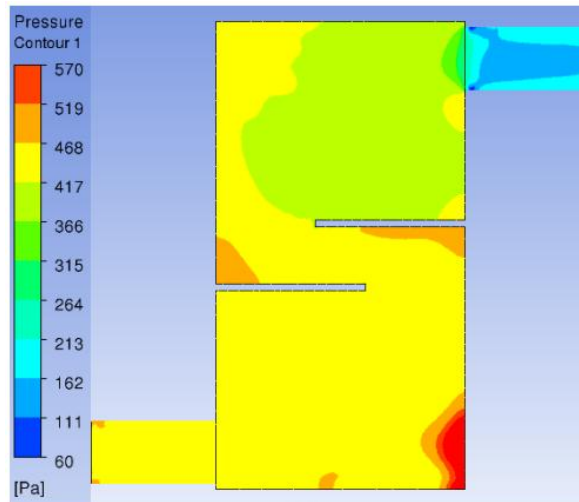


Fig. 25 Pressure contour of vertical scrubber at flow rate $160 [Nm^3/h]$

The pressure drop and streamline distance of a scrubber with two horizontal baffles at baffle length rate of 0.6 are shown in Fig. 18-Fig. 25. Fig. 18 showed that the velocity of gas increased from the inlet pipe to the outlet pipe. The inlet velocity was approximately 7m/s, and the outlet velocity was approximately 11m/s. Fig. 19 showed that the inlet velocity was approximately 11m/s, and the outlet velocity was approximately 16m/s. Fig. 20 showed that the inlet velocity was approximately 13m/s, and the outlet velocity was approximately 18m/s. Fig. 21 showed that the inlet velocity was approximately 17m/s, and the outlet velocity was approximately 23m/s. Fig. 22 showed that the inlet pressure was approximately 100Pa, and the outlet pressure was approximately 60Pa. The pressure decreased from the inlet to the outlet. The pressure of the lower right corner was more than 120Pa, which was the highest. Fig. 23 showed that the inlet pressure was approximately 193Pa, and the outlet pressure was approximately 110Pa. The pressure decreased from the inlet to the outlet. The pressure of the lower right corner was

approximately 235Pa, which was the highest. Fig. 24 showed that the inlet pressure was approximately 310Pa, and the outlet pressure was approximately 210Pa. The pressure decreased from the inlet to the outlet. The pressure of the lower right corner was approximately 380Pa, which was the highest. Fig. 25 showed that the inlet pressure was approximately 468Pa, and the outlet pressure was approximately 315Pa. The pressure decreased from the inlet to the outlet. The pressure of the lower right corner was approximately 570Pa, which was the highest.

2.4 Analysis of scrubber with vertical baffles

2.4.1 Analyzing baffle's length

By using ANSYS to simulate vertical baffle scrubber. The research method is in common with research in horizontal baffle. A pipe of five meters was installed in import and export, respectively, which will make the final results more accuracy. The variable was baffle length. Dividing them into five groups. The baffle length ratio is 0, 0.5, 0.6, 0.7, and 0.8 in each group. The distribution of pressure drop are shown in Table 8, and Fig. 26.

Table 8 Pressure drop of horizontal scrubber with different lengths of baffles

Item [Nm^3/h]	Empty [Pa]	Ratio0.5 [Pa]	Ratio0.6 [Pa]	Ratio0.7 [Pa]	Ratio0.8 [Pa]
Flow Rate- 70	99	142	159	174	218
Flow Rate-100	203	284	320	353	442
Flow Rate-130	330	474	531	593	739
Flow Rate-160	497	713	799	886	1106

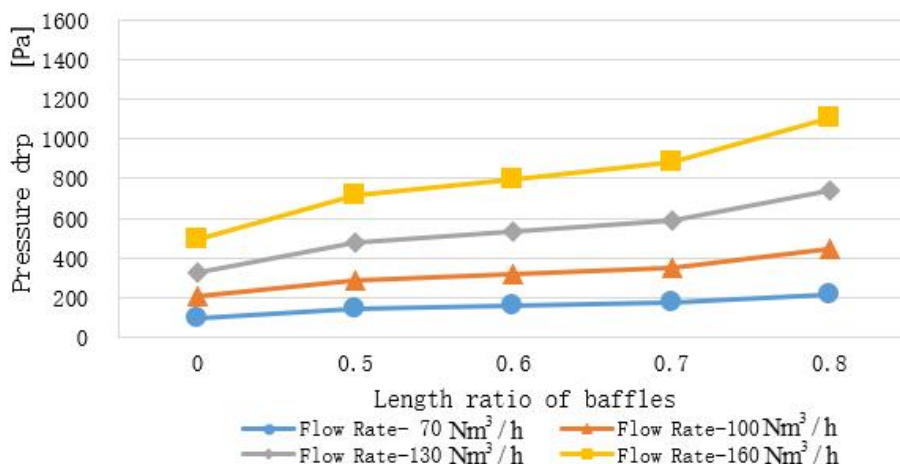


Fig. 26 Pressure drop of horizontal scrubber with different length ratios of baffles

From Table 8 and Fig. 26, at a flow rate of $70 \text{ Nm}^3/\text{h}$, pressure drop of empty scrubber was 99Pa, scrubber at baffle length ratio of 0.8 was 218Pa. The length of baffle increased from 0 to ratio 0.8, and pressure drop had a trend of slow growth. At a flow rate of $100 \text{ Nm}^3/\text{h}$, pressure drop increased from 203 Pa of empty scrubber to 442Pa of length ratio of 0.8. At a flow rate of $130 \text{ Nm}^3/\text{h}$. Pressure drop increased from 330Pa of empty scrubber to 739Pa of scrubber with ratio 0.8. At a flow rate of $160 \text{ Nm}^3/\text{h}$. The pressure drop of empty scrubber was 497Pa, and the pressure drop of scrubber with ratio of 0.8 was 1106Pa. With the increase of baffle length from 0 to ratio 0.8, the values of pressure drop showed an increasing trend. As a whole, under four different flow rates, when the baffle length increased from 0 to ratio 0.7, The pressure drop of the horizontal scrubber showed a slow increasing trend. When the baffle length increased from ratio 0.7 to ratio 0.8, the increasing trend is faster than before. In conclusion, it is better to make the baffle length ratio less than 0.7 when designing this kind of scrubber.

The streamline distance of vertical baffle are shown in Table 9, and Fig. 27.

Table 9 Streamline distance of horizontal scrubber with different length ratios of baffles

Item [Nm^3/h]	Empty [m]	Ratio0.5 [m]	Ratio0.6 [m]	Ratio0.7 [m]	Ratio0.8 [m]
Flow Rate-70	1.21	1.23	1.09	1.71	1.78
Flow Rate-100	1.3	1.26	1.4	1.71	1.73
Flow Rate-130	1.02	1.27	1.28	1.8	1.82
Flow Rate-160	1.22	1.29	1.64	1.49	1.88

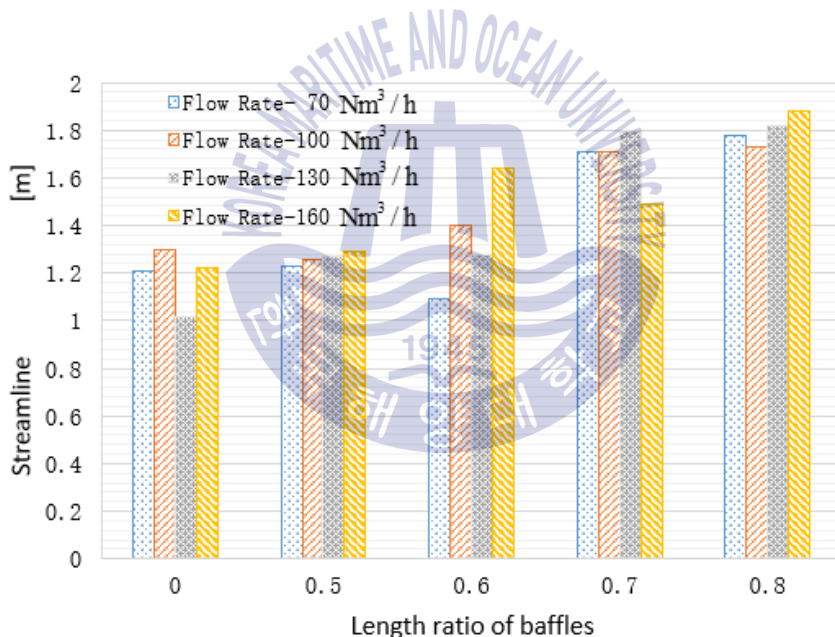


Fig. 27 Streamline distance of horizontal scrubber with different length ratios of baffles

From Table 9 and Fig. 27, at a flow rate of $70Nm^3/h$, the scrubber with baffle length ratio of ratio 0.8 had the longest streamline distance, which was 1.78m. Baffle length ratio of 0.7 was the second long. The minimum value is

the scrubber with baffle length ratio 0.6, which was 1.09m. When the flow rate is $100Nm^3/h$, the maximum streamline distance was baffle length ratio of 0.8, which was 1.73m. The streamline distance of scrubber with length ratio of 0.7 was the second. The minimum value is scrubber with length ratio of 0.5, which was 1.26m. At a flow rate of $130Nm^3/h$, streamline distance of ratio 0.8 is the longest, which was 1.82m. Baffle length ratio of 0.7 was the second long, and the minimum value was the empty scrubber, which was 1.02 m. At a flow rate of $160Nm^3/h$, the maximum streamline distance was 1.88m of scrubber with baffle length ratio 0.8, and the minimum value was 1.22m of the empty scrubber. It could conclude that under four different flow rates, the values of scrubber with baffle length ratio of 0.5, 0.7 and 0.8 are more stable than other cases, and the streamline distances of scrubber with baffle length ratio of 0.7, and 0.8 are longer, which indicated that the two baffle lengths can make the gas-liquid mixture time longer. However, the pressure drop of scrubber with length ratio of 0.8 was large, which will make it lower efficiency energy usage. By combing with the distribution of pressure drop, the results showed that the baffle length ratio of 0.7 is the optimal scheme.

2.4.2 Analyzing baffle's number

It proved that baffle length of ratio 0.7 is the optimal scheme through the former simulation analysis. Baffle length ratio 0.7 was selected in this simulation test. The variable is the baffle number. We divided simulation test into four groups, the number of baffles in each group are 0, 2, 4, and 6, respectively. ANSYS were used for four groups of simulation tests. The pressure drop of scrubber with different numbers of vertical baffles are shown in Table 10, and Fig. 28.

Table 10 Pressure drop of horizontal scrubber with different numbers of baffles

Item [Nm^3/h]	Empty [Pa]	2-Baffles [Pa]	4-Baffles [Pa]	6-Baffles [Pa]
Flow Rate- 70	99	174	238	309
Flow Rate-100	203	353	479	630
Flow Rate-130	330	593	811	1070
Flow Rate-160	497	886	1209	1621

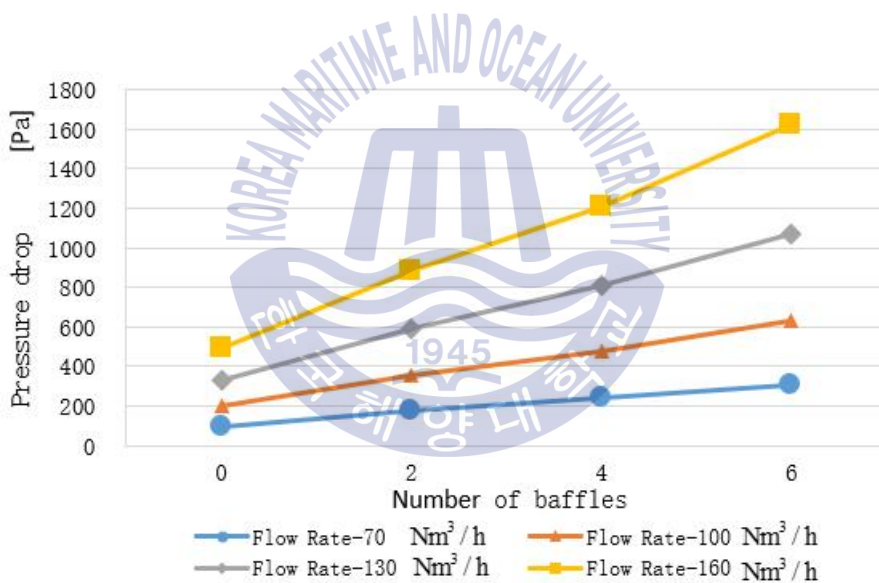


Fig. 28 Pressure drop of horizontal scrubber with different numbers of baffles

From Table 10 and Fig. 28, at four different flow rates, when baffle length increases from 0 to 6, The pressure drop value of scrubber shows an increasing trend. The bigger flow rate it is, the higher increasing trend is. Pressure drop indicates power efficiency. Smaller pressure drop makes higher

power efficiency. When designing this type of scrubber, the baffle length should not be excessive. The streamline distance were calculated by ANSYS and were shown in Table 11 and Fig. 29.

Table 11 Streamline distance of horizontal scrubber with different numbers of baffles

Item [Nm^3/h]	Empty [m]	2-Baffles [m]	4-Baffles [m]	6-Baffles [m]
Flow Rate- 70	1.21	1.71	1.4	1.45
Flow Rate-100	1.3	1.71	1.65	1.19
Flow Rate-130	1.02	1.8	1.78	1.24
Flow Rate-160	1.22	1.49	1.8	1.04

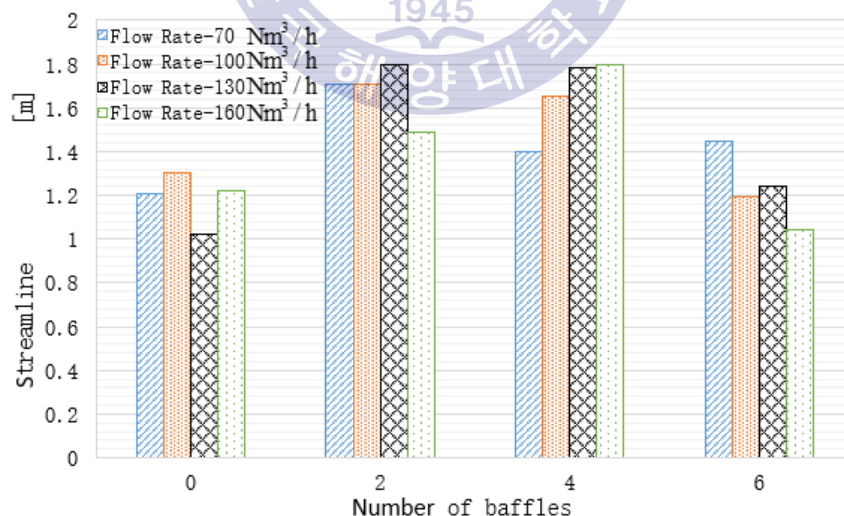


Fig. 29 Streamline distance of horizontal scrubber with different numbers of baffles

It can be seen from Table 11 and Fig. 29, when the flow rate is $70Nm^3/h$, the maximum streamline distance is scrubber with 2 baffles, which is 1.71m. Scrubber with 6 baffles is the second, which is 1.45m. Scrubber with 4 baffles is 1.4m. The minimum streamline distance is the empty scrubber, which is 1.21m. When the flow rate is $100Nm^3/h$, the maximum streamline distance is scrubber with 2 baffles, which is 1.71m. the streamline distance of scrubber with 4 baffles is the second, which is 1.65m. scrubber with 6 baffles is the smallest, which is 1.19m. When the flow rate is $130Nm^3/h$, streamline distance with 2 baffles is maximum, which is 1.8m. Scrubber with 4 baffles is the second, which is 1.78m. The empty scrubber is the minimum, which is 1.02m. When the flow rate is $160Nm^3/h$, streamline distance of scrubber with 4 baffles is the maximum, which is 1.8m. Scrubber with 6 baffles is the smallest, which is 1.04m. It can be seen that the streamline distance of scrubber with 2 and 4 baffles are longer and more stable than other cases. It shows that the scrubber has better washing effect when the streamline distance is longer. Combining with the diagram of pressure drop, It can conclude that when designing this type of scrubber, the baffle length of ratio 0.7 and 2 baffles was the optimal scheme.

Chapter 3 Investigation on the performance of sprays in a small scrubber for marine engines

3.1 Mathematical model and conditions

3.1.1 Structure of scrubbers

According to the “The International Convention for the Prevention of Pollution From Ships” published by International Maritime Organization (IMO) on January 1st, 2015. The convention stipulated that the allowable emissions of sulphur oxides from ships in the Global Emission Control Area (ECA) will be reduced from 1% to 0.1%. As a result, ship operators must take measures to reduce sulfur oxide emissions. Installing marine exhaust scrubber is the best measure with the lowest cost and higher efficiency. Through a series of chemical and physical reactions, Scrubber can wash out and remove the main pollutant, such as NO_x , SO_x and particulates produced by diesel engines. In this research, a kind of scrubber for small marine engine was simulated and analyzed two important parameters (inlet pressure and streamline). The influence of the nozzle location and number on the washing effect and power utilization efficiency was discussed. The optimal inner structure was found out after fluid analysis of the scrubber for small marine engine.

Marine fuel drops SO_x , NO_x and particulates into the atmosphere during combustion, which not only pollutes the atmosphere, but also endangers human health. According to the MARPOL Annex VI [18]-[20] adopted in 2011, from 2015, in North America, the Baltic Sea, the North Sea and the Caribbean Maritime Space, reducing the upper limit of SO_x emissions for marine vessels from 1% to 0.1%, and the upper limit of SO_x emission standards for ships will be reduced to 0.5% in all European sea areas except

ECA. The emission standard for SO_x will be further reduced to 0.1% by 2020, and the new regulation of 0.5% SO_x emissions by 2020 or 2025 will come into effect globally. There are three main control measures for marine SO_x emission including using low sulfur oil, replacing the dual fuel engine and installing the exhaust gas scrubber. Liang et al testified the n-tetradecane-toluene mechanism including 30% mass fraction toluene is most suitable as a surrogate fuel for a marine diesel engine [21]. Byeong-Yong Yoo assessed the cost competition of liquefied natural gas (LNG) is better than marine gas oil (MGO) as a marine fuel [22]. Belgiorna et al investigated the single effects of the compression ratio and of the main engine calibration parameters after updated the combustion architecture of dual fuel engine [23]. Installation of waste gas scrubber is the most cost-effective method. Galarraga et al applied a stochastic model to find that the remaining lifetime and sailing time in ECAs of vessels are the determinant factors to install a scrubber rather than switching fuel [24]. In order to accompany the requirements of relevant international regulations, many shipping lines and institutions are researching how to improve the efficiency of dust removal and desulfurization technology of various types of scrubbers [25]-[32].

This research based on D4AK-C diesel engine, which investigated on two phases flow of the effects of nozzles on the flow performance. The 3D-view modeling was set up by NX 9.0 and the fluid simulation of scrubber was carried out by ANSYS. By changing the position and quantity of nozzles inside the scrubber and controlling the total flow rate of washing liquid, it found out the relations among pressure drop and streamline with power efficiency and washing effect of the scrubber under four engine working velocities. It concluded the optimal inner structure of the small scrubber for marine engine after simulation and analysis.

Volume of the small scrubber for marine engine is 60L, 1000mm in length, 300mm in width and 200mm in height. Fluid simulation was carried out under four working velocities of D4AK-C diesel engine. The simulated exhaust gas is Vapor Model with a gas-liquid ratio of 99:1. The nozzle radius is 5mm, the injection angle is 60° and the total particle mass flow rate is 0.001 kg/s. All the two-dimensional views and three-dimensional views are drawn by NX 9.0. The sectional view, 3D-view and mesh view of the small scrubber for marine engine are shown in Fig. 30, Fig. 31 and Fig. 32.

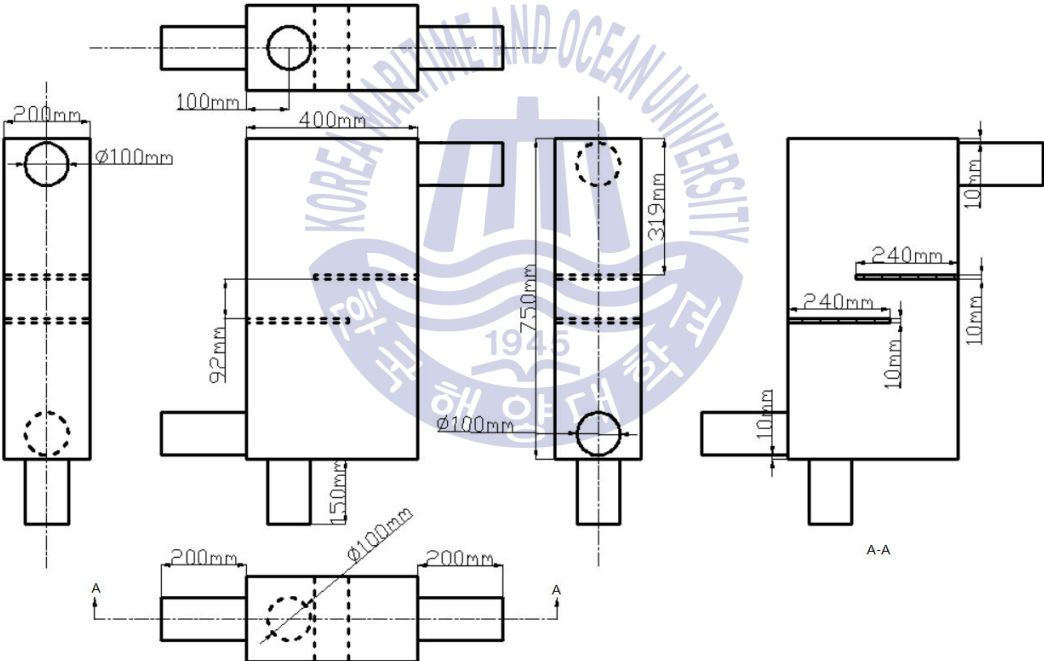


Fig. 30 Sectional view of vertical scrubber

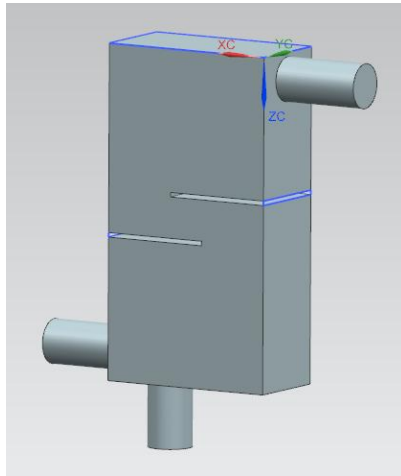


Fig. 31 3D-view of vertical scrubber



Fig. 32 Mesh view of vertical scrubber

The scrubber is divided into air inlet pipe (down left side), air outlet pipe (upper right side), water outlet pipe (down side) and washing room. Exhaust gas enters from inlet pipe and out from the outlet pipe; the washing liquid falls down after washing progress in virtue of gravity and is discharged from the water outlet pipe.

3.1.2 Boundary conditions

The exhaust gas is exported from D4AK-C diesel engine. The parameters of D4AK-C diesel engine are shown in Table 12. The working velocities of D4AK-C diesel engine and the corresponding exhaust gas flow rates and velocities are shown in Table 13.

Table 12 Specifications of “D4AK-C” diesel engine

Type	Turbo diesel engine (D4AK-C)
Cooling method	Water cooler
No.of cyl.& arrangement	4-IN line
Valve mechanism	Overhead valve
Combustion chamber type	Direct injection
Bore × stroke	100mm × 105mm
Total piston displacement	3298cc
Compression ratio	16:1
Rated output(KSR 1004)	80/2400(ps/rpm)
NO-load minimum Speed	700-750rpm
NO-load Maximum Speed	2640 ± 20rpm
Firing order	1-3-4-2
Injection timing	16° ± 1° BTDC

Table 13 Engine speed and gas flow rate

Engine Speed (rpm)	700	1000	1300	1600
Flow rate (Nm^3/h)	70	100	130	160
Inlet speed (m/s)	7.44	10.62	13.8	16.98
Number of mesh	1229282			
Number of node	208258			
Number of nozzle	2	Length (mm)		240

Mesh files were set up by ICEM CFD. The mesh elements and nodes were generated as the same number in order to reduce the mesh effect on calculation. Volume Mesh was adopted, and the mesh type was Tetra/Mixed. The unit of mesh was 0.009. It kept mesh number more than two million and remained good performance of final results. The total mesh elements were 1229282, the total nodes were 208258. Using ANSYS to simulate and calculate after grid division. It kept residual target in $1.0E-0.6$. The simulation results were arithmetic means due to the turbulent flow.

3.2 Simulation and calculation results

3.2.1 Calculation conditions

The simulation was carried out in two groups. The variable is the position of nozzle. It took two conical nozzles, the nozzle radius was 5mm, and the injection velocity was 15m/s. Fixing the injection angle in 60 degrees. and total particle mass flow rate in 0.001kg/s. The first simulation model put the two nozzles on the wall horizontally. The second model places the two nozzles on the top of wall and front of one baffle vertically. The specification of

nozzles is shown in Table 14, the two groups of models are shown in Fig. 33 and Fig. 34, respectively. Exhaust gas get into scrubber from the down left pipe, and get out from the up right pipeline. Washing liquid dropped out from the pipeline on the bottom. It took water as washing liquid of the analog simulation.

Table 14 Specifications of nozzles in research of nozzle location

Type	Full cone	
Injection velocity (m/s)	15	
Cone angle (°)	60°	
Particle diameter (μm)	5	
Total mass flow rate (kg/s)	0.001	
Number of nozzles	Horizontal	2
	Vertical	

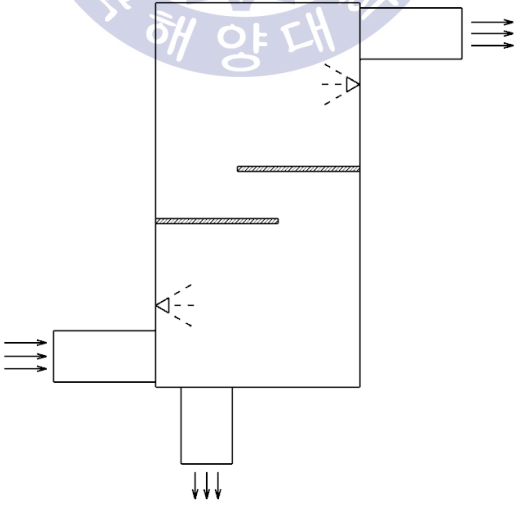


Fig. 33 Distribution of horizontal nozzles

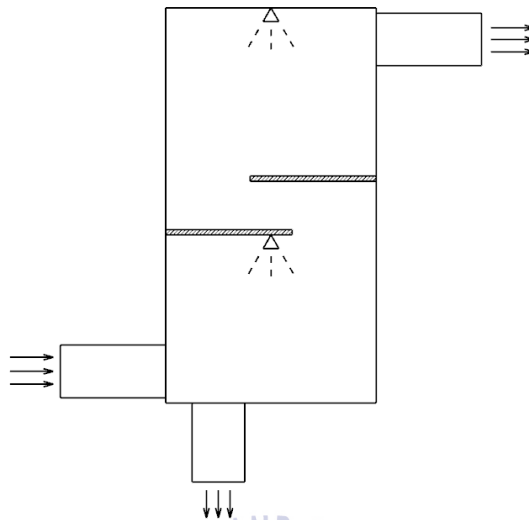


Fig. 34 Distribution of vertical nozzles

3.2.2 Analysing locations of nozzles

Pressure drop features the power utilization efficiency of diesel engines. The lower inlet pressure is, the higher power utilization is. Pressure distribution of scrubber with vertical and horizontal nozzles are show from Fig. 35 to Fig. 42. Histogram of inlet pressures are shown in Fig. 43. At a flow rate of $70Nm^3/h$, the inlet pressure of scrubber with horizontal nozzles was 25Pa, scrubber with vertical nozzles was 24Pa. At a flow rate of $100Nm^3/h$, scrubber with horizontal nozzles was 55Pa, and scrubber with vertical nozzles was 54Pa. At a flow rate of $130Nm^3/h$, the pressure drop of scrubber with horizontal nozzles was 95Pa, scrubber with vertical nozzles was 96Pa. At a flow rate of $160Nm^3/h$, scrubber with horizontal nozzles was 148Pa, and scrubber with vertical nozzles was 147Pa.

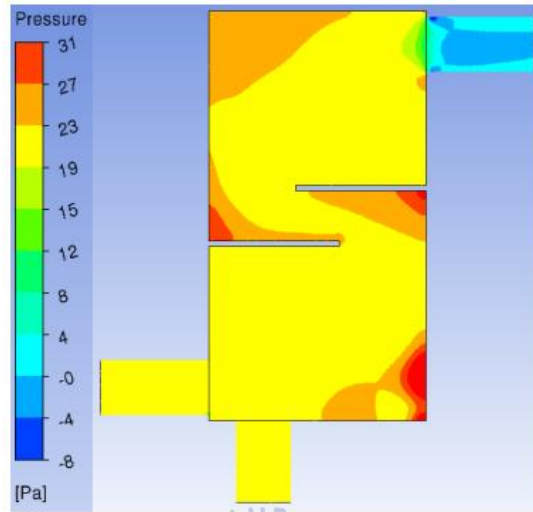


Fig. 35 Pressure contour of vertical nozzles at flow rate 70 [Nm^3/h]

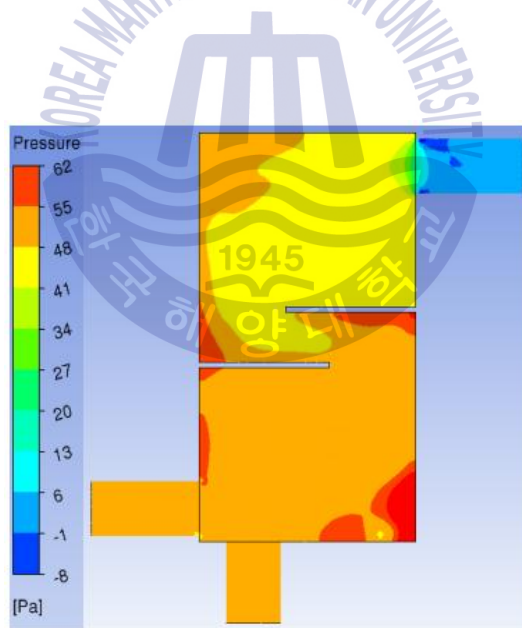


Fig. 36 Pressure contour of vertical nozzles at flow rate 100 [Nm^3/h]

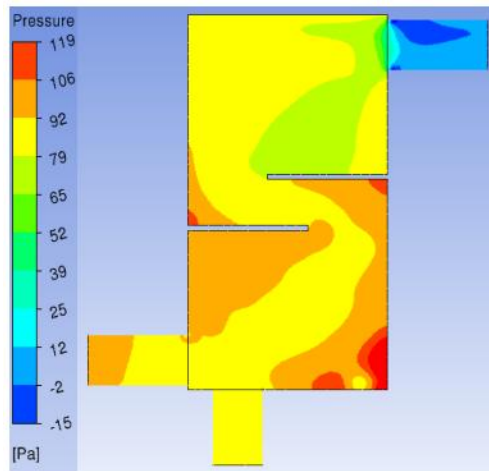


Fig 37 Pressure contour of vertical nozzles at flow rate 130 [Nm^3/h]

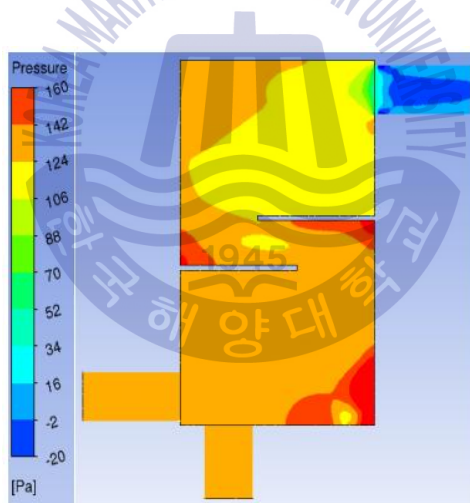


Fig. 38 Pressure contour of vertical nozzles at flow rate 160 [Nm^3/h]

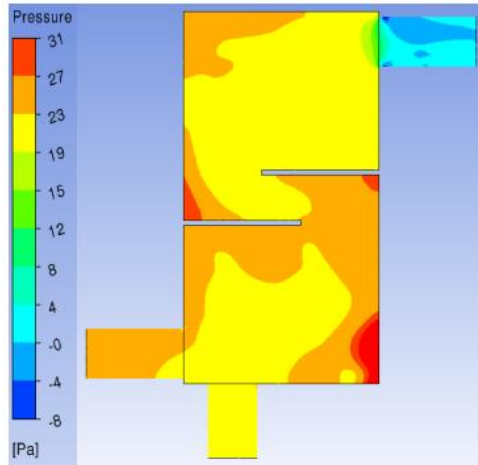


Fig. 39 Pressure contour of horizontal nozzles at flow rate 70 [Nm^3/h]

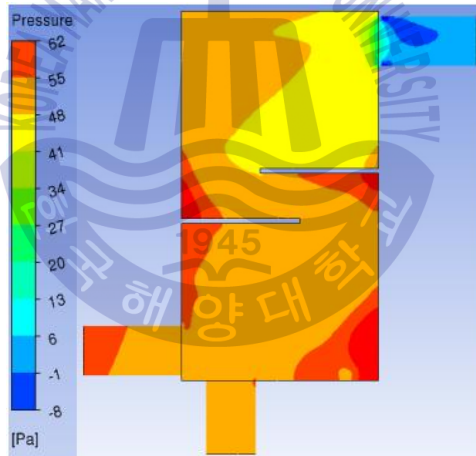


Fig. 40 Pressure contour of horizontal nozzles at flow rate 100 [Nm^3/h]

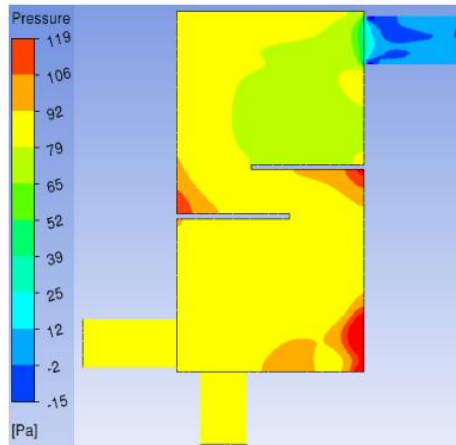


Fig. 41 Pressure contour of horizontal nozzles at flow rate 130 [Nm^3/h]

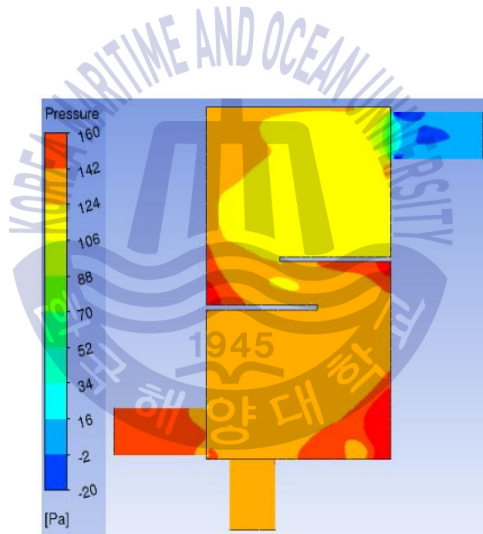


Fig. 42 Pressure contour of horizontal nozzles at flow rate 160 [Nm^3/h]

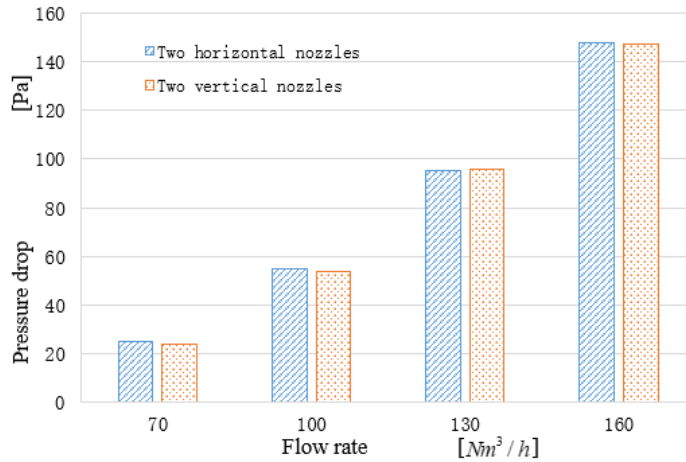


Fig. 43 Comparison of pressure drop

As shown in Fig. 43, the red histogram indicated scrubber with vertical nozzles, and the blue one represented scrubber with horizontal nozzles. According to Fig. 43, the inlet pressure increased with the growth of gas flow rate, and the inlet pressure of two scrubbers was approximately same at each flow rate. It indicated that there is little effect on inlet pressure of these two schemes. The power utilization of these two cases were no apparent different.

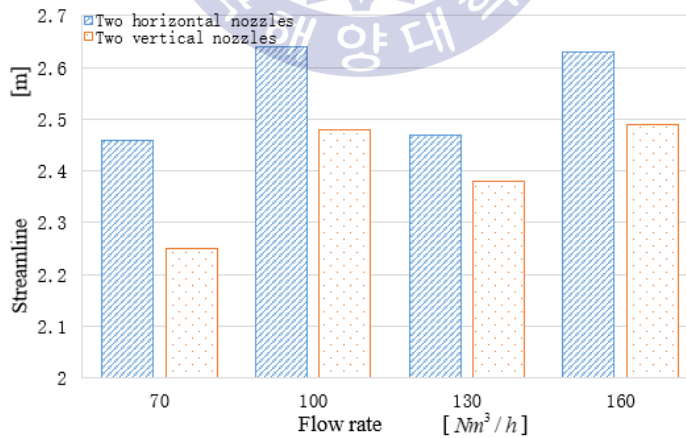


Fig. 44 Comparison of streamline distance

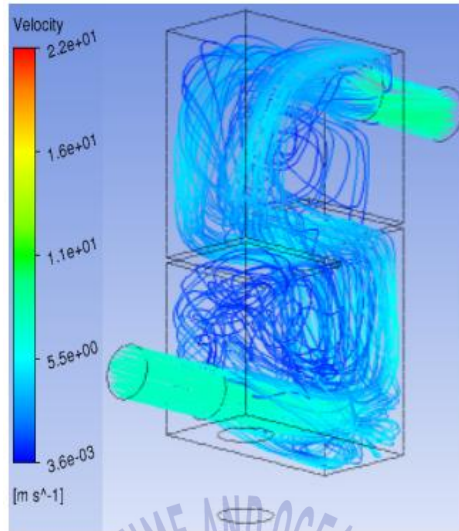


Fig. 45 Streamline distance of vertical nozzles at flow rate 70 [Nm^3/h]

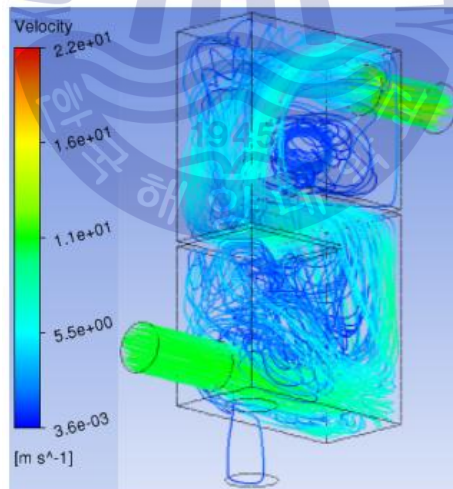


Fig. 46 Streamline distance of vertical nozzles at flow rate 100 [Nm^3/h]

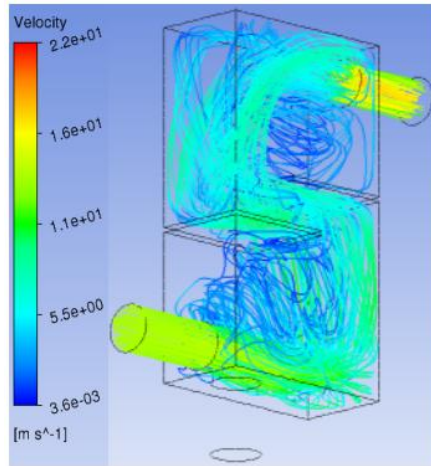


Fig. 47 Streamline distance of vertical nozzles at flow rate 130 [Nm^3/h]

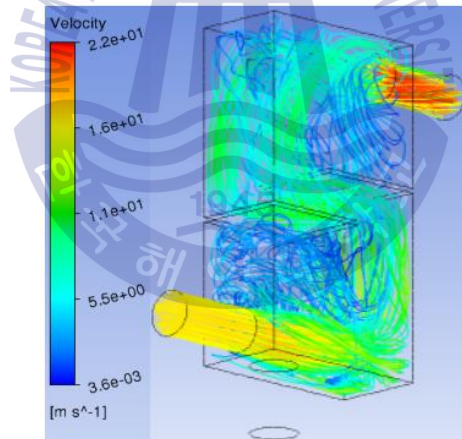


Fig. 48 Streamline distance of vertical nozzles at flow rate 160 [Nm^3/h]

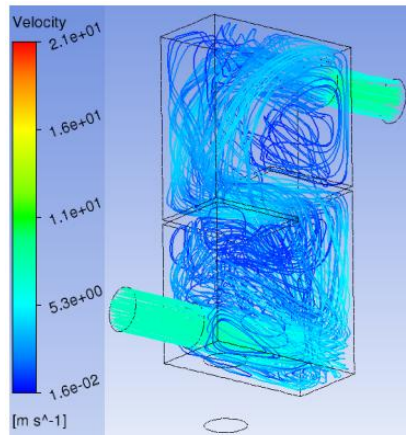


Fig. 49 Streamline distance of horizontal nozzles at flow rate 70 [Nm^3/h]

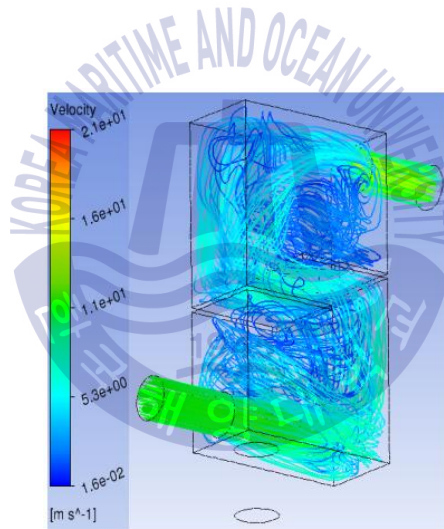


Fig. 50 Streamline distance of horizontal nozzles at flow rate 100 [Nm^3/h]

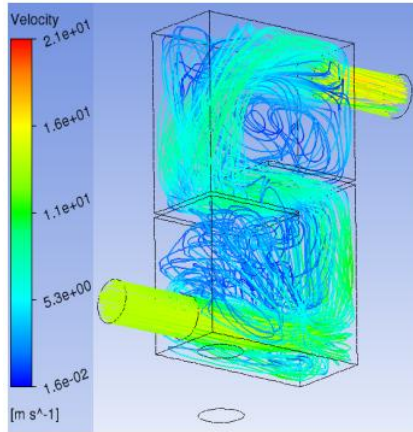


Fig. 51 Streamline distance of horizontal nozzles at flow rate 130 [Nm^3/h]

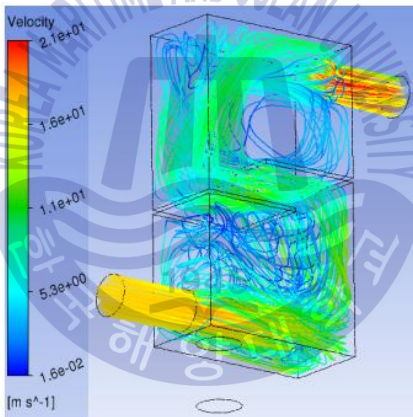


Fig. 52 Streamline distance of horizontal nozzles at flow rate 160 [Nm^3/h]

Streamline distance is a fact to measure washing effect. The larger streamline distance indicates the longer mixing time of exhaust gas and detergent. Fig. 44 was a diagram of scrubbers with different direction of nozzles. The blue histogram represented scrubber with horizontal nozzles, and the red one was vertical nozzles. At a flow rate of $70Nm^3/h$, Streamline of horizontal nozzles was 2.45m, and streamline of vertical nozzles was 2.25m. At a flow rate of $100Nm^3/h$, streamline of horizontal nozzles was 2.6m, and the value of vertical nozzle was 2.48m. At a flow rate of $130Nm^3/h$, streamline values of horizontal and vertical nozzles scrubber were 2.52m and 2.38m, respectively. At a flow rate of $160Nm^3/h$, streamline of horizontal nozzle was 2.63m, and the vertical one was 2.49m. According to Fig. 44, streamline distance of the scrubber with horizontal nozzles are higher than that of vertical nozzles under four flow rates. It could conclude that to install nozzles horizontally has a better washing effect comparing with vertical one. Streamlines distribution of these two scrubbers are shown from Fig. 45 to Fig. 52.

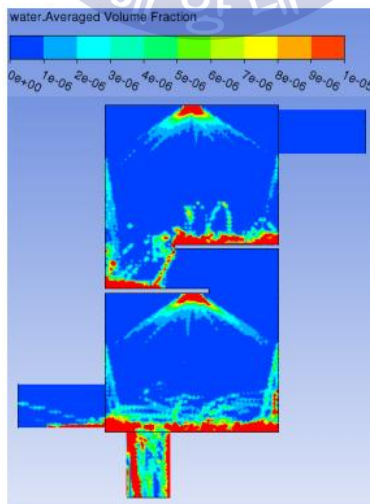


Fig. 53 Water distribution of vertical nozzles at flow rate 70 [Nm^3/h]

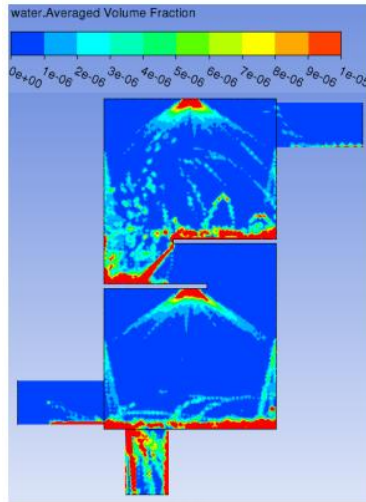


Fig. 54 Water distribution of vertical nozzles at flow rate 100 [Nm^3/h]

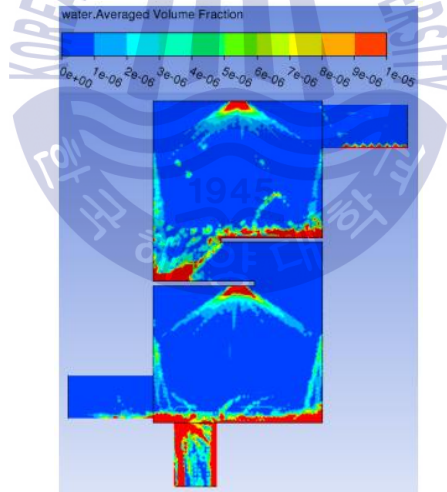


Fig. 55 Water distribution of vertical nozzles at flow rate 130 [Nm^3/h]

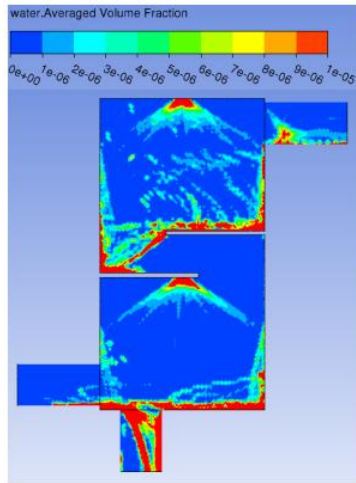


Fig. 56 Water distribution of vertical nozzles at flow rate 160 [Nm^3/h]

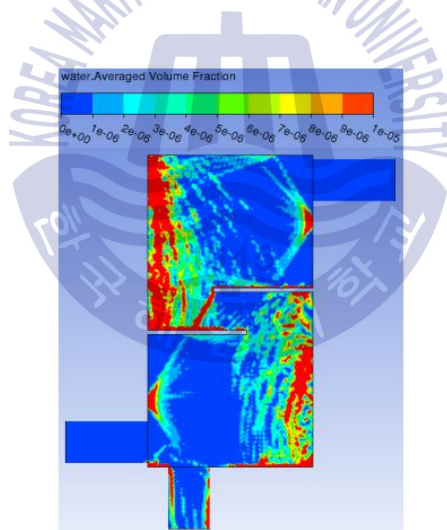


Fig. 57 Water distribution of horizontal nozzles at flow rate 70 [Nm^3/h]

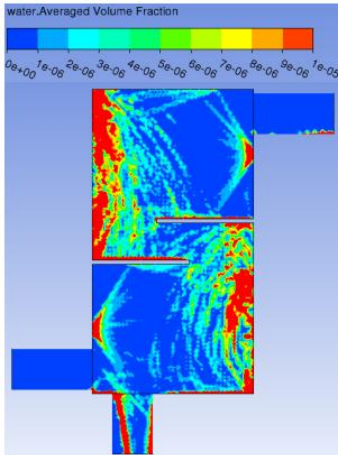


Fig. 58 Water distribution of horizontal nozzles at flow rate 100 [Nm^3/h]

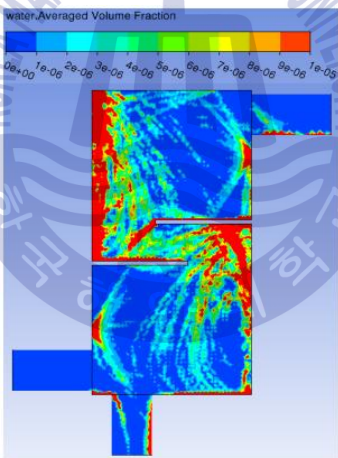


Fig. 59 Water distribution of horizontal nozzles at flow rate 130 [Nm^3/h]

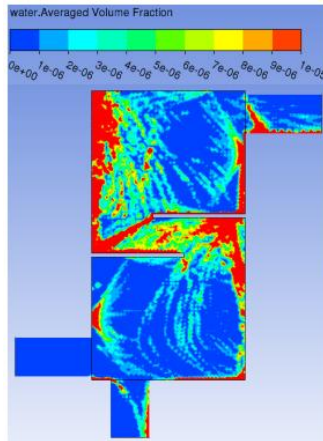


Fig. 60 Water distribution of horizontal nozzles at flow rate 160 [Nm^3/h]

The water volume fraction distributions of two scrubbers are shown in Fig. 53–Fig. 60. Fig. 53–Fig. 56 were the scrubbers with vertical nozzles, and Fig. 57–Fig. 60 were the scrubbers with horizontal nozzles. Under four gas flow rates, water in the scrubbers with vertical nozzles was concentrated on the upper surface of baffles, but there was no washing liquid on the bottom space of baffles. Water in the scrubbers with horizontal nozzles was well-distributed, which filled with water in the whole cavity, and vapor distribution was more concentrated on the wall. It concluded that the washing effect was better on horizontal nozzles than vertical nozzles.

3.2.3 Analyzing numbers of nozzles

According to the first simulation results, small scrubber for marine engine with volume of 60L, streamline was larger of horizontal nozzles than vertical one. Vapor distribution has a better performance of horizontal nozzles. There was no big difference between two schemes. Variable was nozzle number in the second group of analog simulation. Employing conical nozzle with radius of

5mm horizontally. Fixing the spray angle in 60° , and total particle mass flow rate in 0.001kg/s. From two to eight nozzles were installed in seven scrubbers, respectively. The specifications of nozzles are shown in Table 15. The distributions of nozzles are shown in Fig. 61-Fig. 67.

Table 15 Specifications of nozzles in research of nozzle number

Type	Full cone						
Injection velocity (m/s)	15						
Cone angle ($^\circ$)	60°						
Particle diameter (μm)	5						
Total mass flow rate (kg/s)	0.001						
Number of nozzles	2	3	4	5	6	7	8

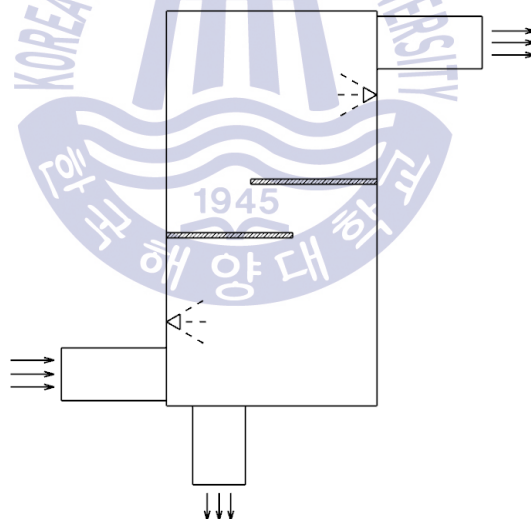


Fig. 61 Distribution of two horizontal nozzles

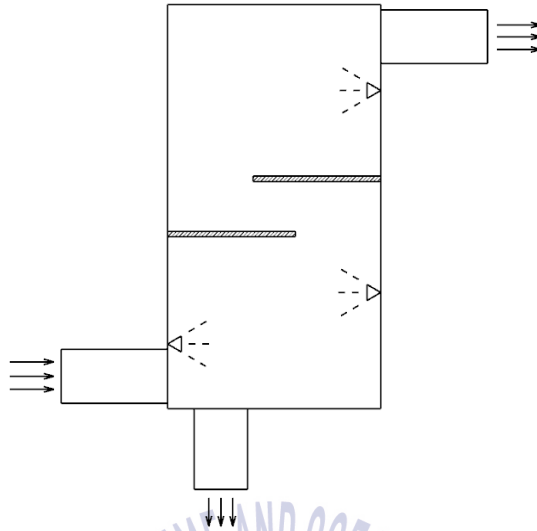


Fig. 62 Distribution of three horizontal nozzles

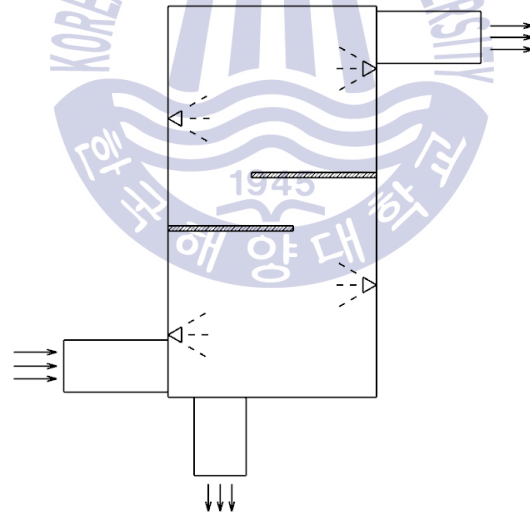


Fig. 63 Distribution of four horizontal nozzles

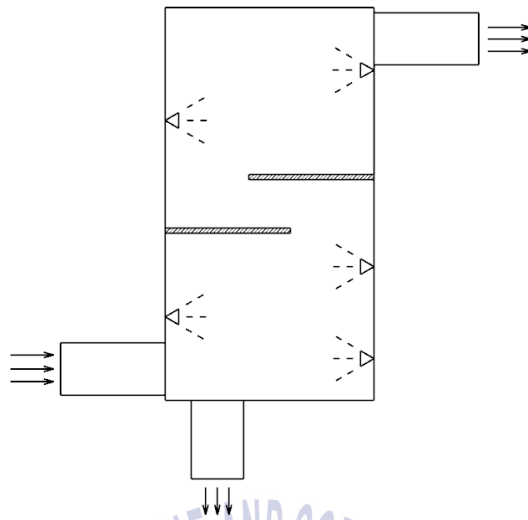


Fig. 64 Distribution of five horizontal nozzles

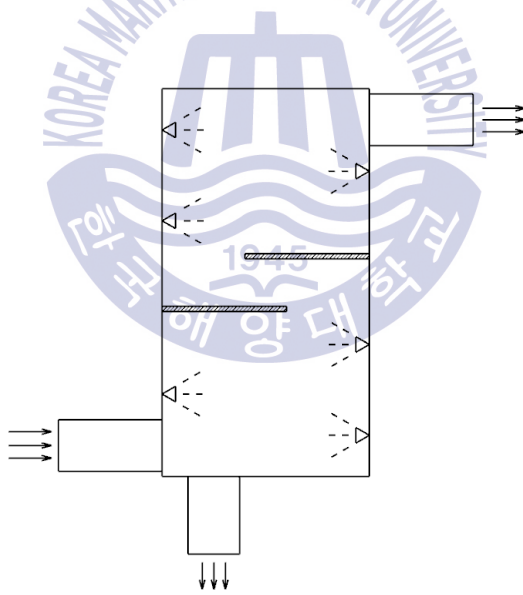


Fig. 65 Distribution of six horizontal nozzles

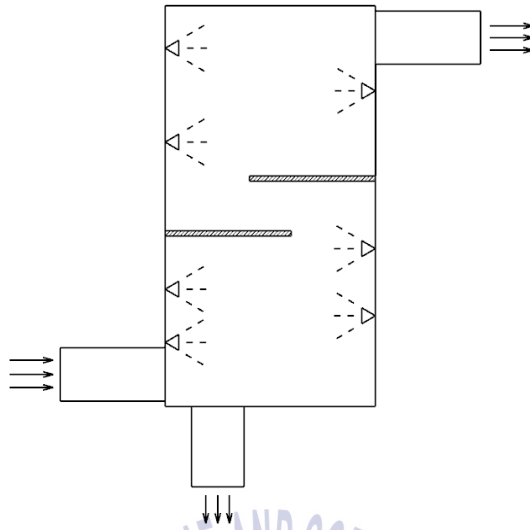


Fig. 66 Distribution of seven horizontal nozzles

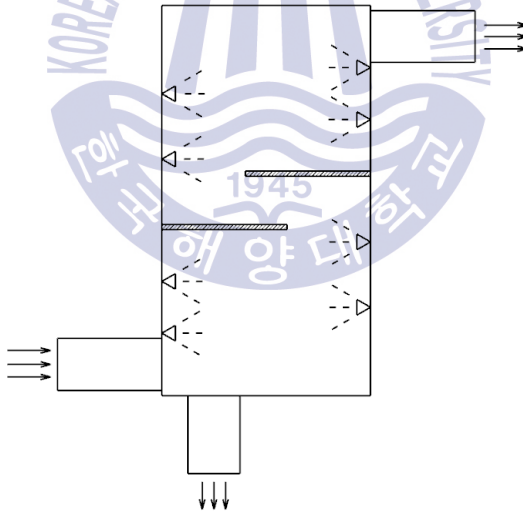


Fig. 67 Distribution of eight horizontal nozzles

After analysing scrubber with different number of nozzles, it got the values about inlet pressure, which is shown in Table 16.

Table 16 Pressure drop of scrubber with different number of nozzles

	70 [Nm ³ /h]	100 [Nm ³ /h]	130 [Nm ³ /h]	160 [Nm ³ /h]
2-nozzles	24Pa	54Pa	96Pa	148Pa
3-nozzles	24Pa	54Pa	96Pa	148Pa
4-nozzles	24Pa	54Pa	96Pa	147Pa
5-nozzles	24Pa	55Pa	95Pa	147Pa
6-nozzles	24Pa	55Pa	96Pa	147Pa
7-nozzles	24Pa	55Pa	97Pa	148Pa
8-nozzles	24Pa	55Pa	96Pa	148Pa

According to Table 16, at a flow rate of 70Nm³/h, the inlet pressure values of scrubbers were all 24Pa. At a flow rate of 100Nm³/h, the inlet pressure of scrubbers with 2, 3, and 4 nozzles were 54Pa, scrubber with 5, 6, 7 and 8 were 55Pa. At a flow rate of 130Nm³/h, the inlet pressure of scrubbers with 2, 3, 4, 6, 8 were 96Pa. The value of scrubber with 5 nozzles was 95Pa. The value of scrubber with 7 nozzles were 9 Pa. At a flow rate of 160Nm³/h, the inlet pressure of scrubber with 2, 3, 7, 8 nozzles were 148Pa. The value of scrubber with 4, 5, 6 nozzles were 147Pa. It is indicated that there was little change on pressure drop when enhancing the number of nozzles and keeping total particle mass flow rate in constant. The power utilization was similar of scrubbers with different numbers of nozzles.

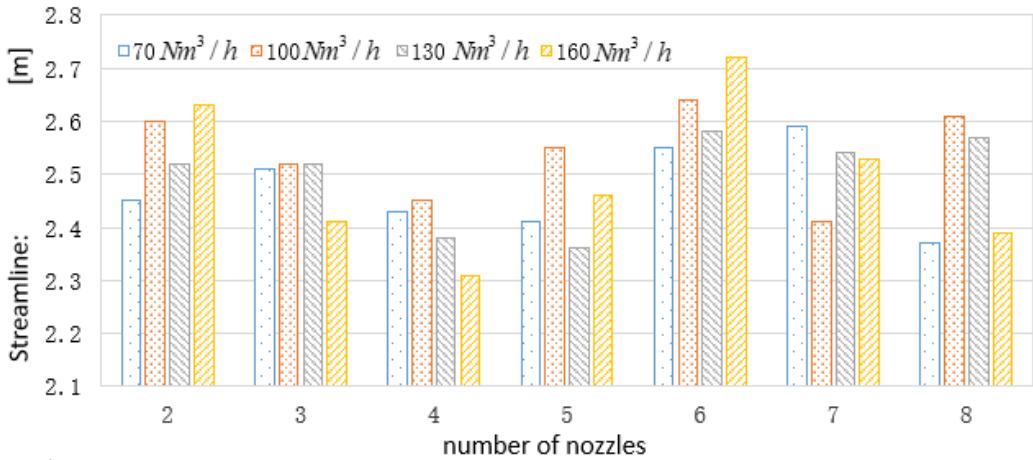


Fig. 68 Streamline distance with different numbers of horizontal nozzles

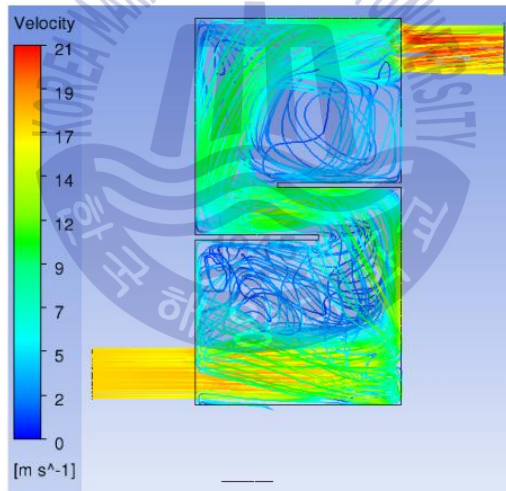


Fig. 69 Streamline distribution of two horizontal nozzles at flow rate 160 [Nm^3/h]

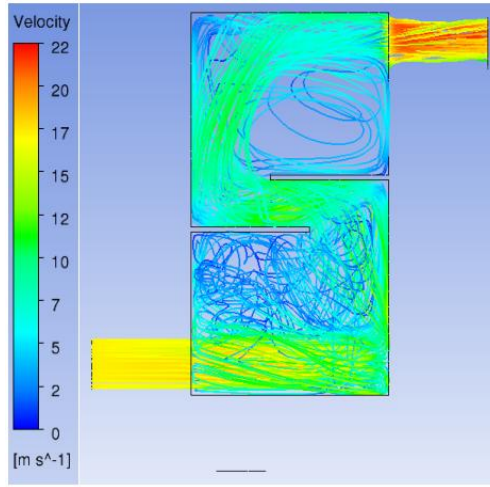


Fig. 70 Streamline distribution of three horizontal nozzles at flow rate $160 \text{ [Nm}^3/\text{h}]$

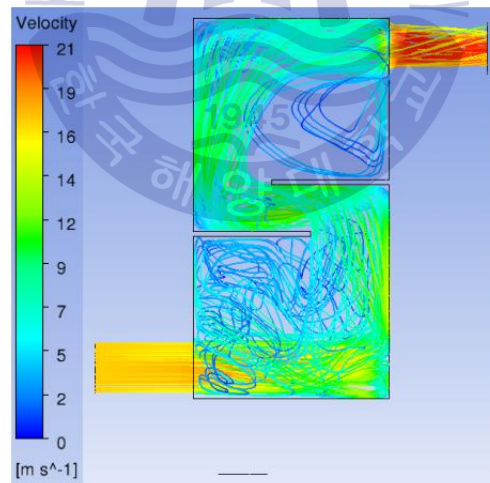


Fig. 71 Streamline distribution of four horizontal nozzles at flow rate $160 \text{ [Nm}^3/\text{h}]$

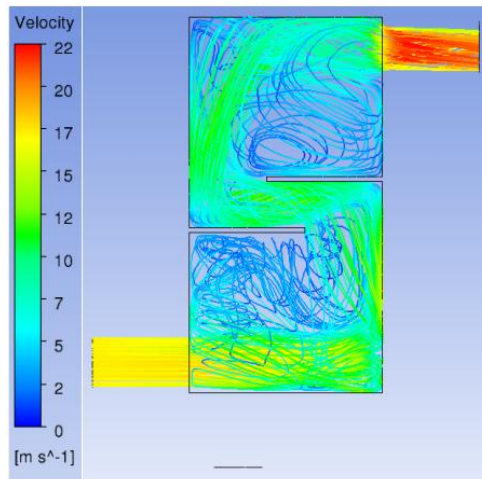


Fig. 72 Streamline distribution of five horizontal nozzles at flow rate 160 [Nm^3/h]

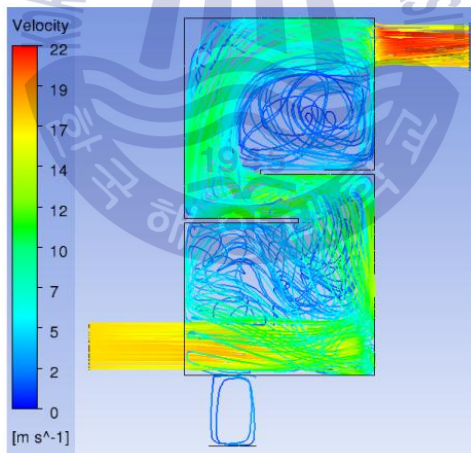


Fig. 73 Streamline distribution of six horizontal nozzles at flow rate 160 [Nm^3/h]

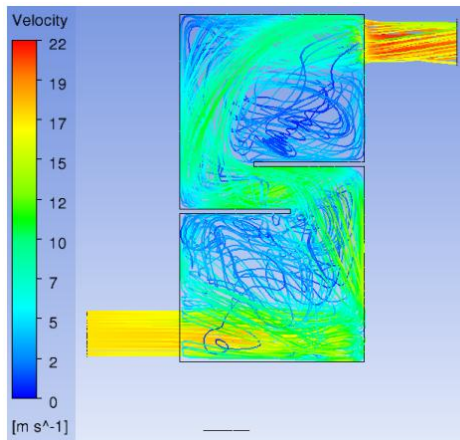


Fig. 74 Streamline distribution of seven horizontal nozzles at flow rate 160 [Nm^3/h]

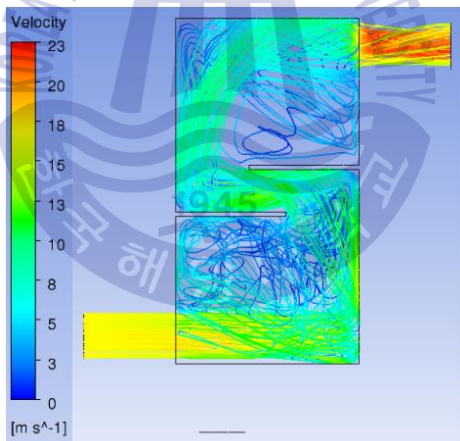


Fig. 75 Streamline distribution of eight horizontal nozzles at flow rate 160 [Nm^3/h]

By analyzing the average flow distance, the streamline distribution of all scrubbers was obtained as shown in Fig. 68. According to Fig. 68, histograms in different colours indicated different gas flow rates. The streamline distance was not much dependent on the flow rate. The streamline distance decreased with number of nozzle increased until 4, and then increased until 4 nozzles, the streamline distance decreased from 6 nozzles to 8 nozzles. On the whole, the streamline distance of scrubber with 6 horizontal nozzles was the longest, which indicated that scrubber with 6 horizontal nozzles has the longest mixing time of water and exhaust gas. It had the best washing effect under flow rates. Here are the streamline distribution shown in Fig. 69–Fig. 75.

3.2.4 The optimal structure

According to the former discussion, the scrubber with 6 horizontal nozzles were found to be the optimal inner structure. Here are the distributions of water shown in Fig. 76–Fig. 79.

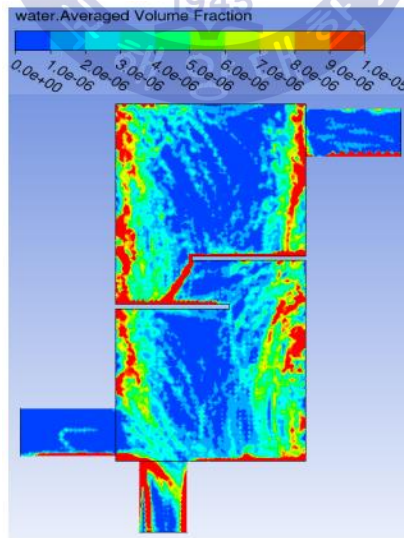


Fig. 76 Water distribution of six horizontal nozzles at flow rate 70 [Nm^3/h]

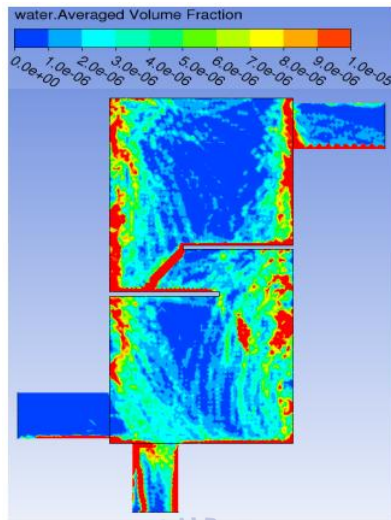


Fig. 77 Water distribution of six horizontal nozzles at flow rate 100 [Nm^3/h]

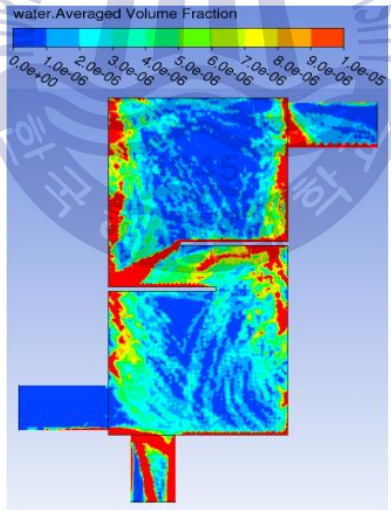


Fig. 78 Water distribution of six horizontal nozzles at flow rate 130 [Nm^3/h]

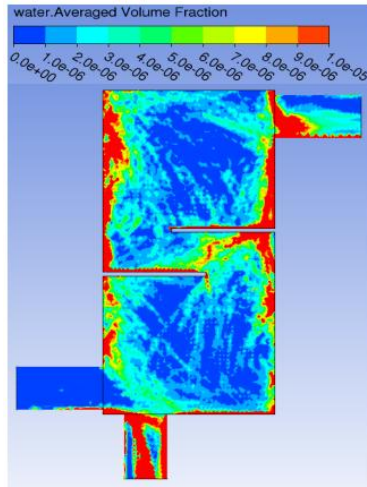


Fig. 79 Water distribution of six horizontal nozzles at flow rate 160 [Nm^3/h]

Fig. 76-Fig. 79 showed the water distribution in scrubber with 6 horizontal nozzles. Water distribution was homogeneous under four flow rates. The chambers were full of water, and water was concentrate on the walls and corners of scrubbers.

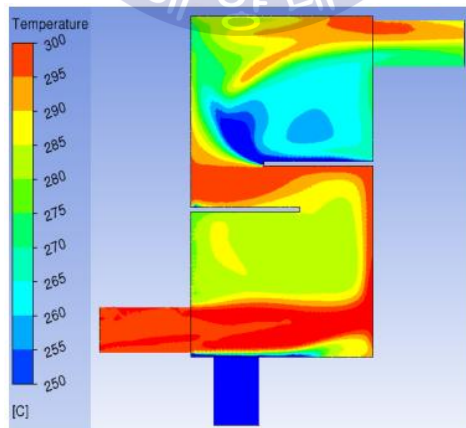


Fig. 80 Temperature of six horizontal nozzles at flow rate 70 [Nm^3/h]

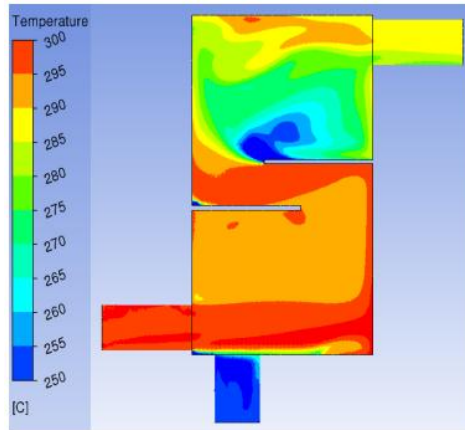


Fig. 81 Temperature of six horizontal nozzles at flow rate 100 [Nm^3/h]

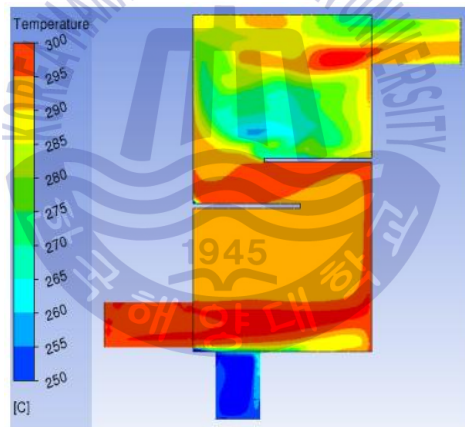


Fig. 82 Temperature of six horizontal nozzles at flow rate 130 [Nm^3/h]

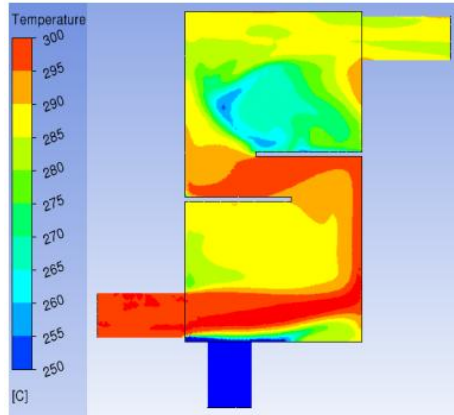


Fig. 83 Temperature of six horizontal nozzles at flow rate 160 [Nm^3/h]

Fig. 80-Fig. 83 showed the inlet temperature of scrubber under four flow rates was about 300°C, the outlet temperature at 70 Nm^3/h was about 285°C, the outlet temperature at 100 Nm^3/h was about 286°C, the outlet temperature at 130 Nm^3/h was about 290°C, the outlet temperature at 160 Nm^3/h was about 286°C. Fig. 80 -Fig. 83 showed the temperature of gas was high around the inlet pipe, and kept low level around the upper baffle. There was no big difference in temperature between inlet pipe and outlet pipe.

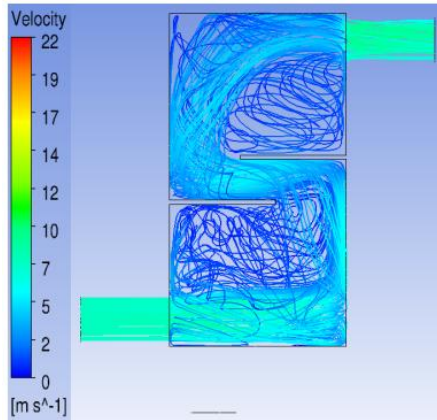


Fig. 84 Streamline of six horizontal nozzles at flow rate 70 [Nm^3/h]

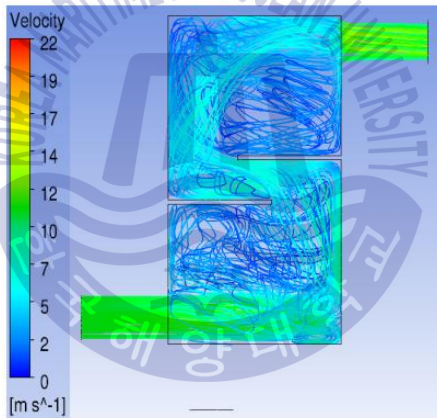


Fig. 85 Streamline of six horizontal nozzles at flow rate 100 [Nm^3/h]

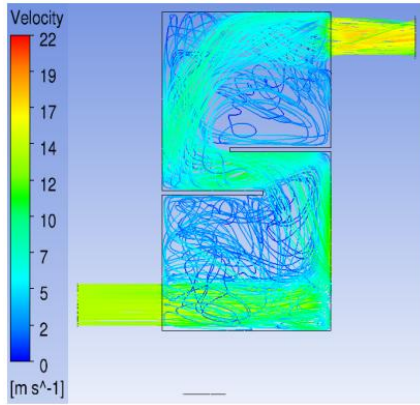


Fig. 86 Streamline of six horizontal nozzles at flow rate 130 [Nm^3/h]

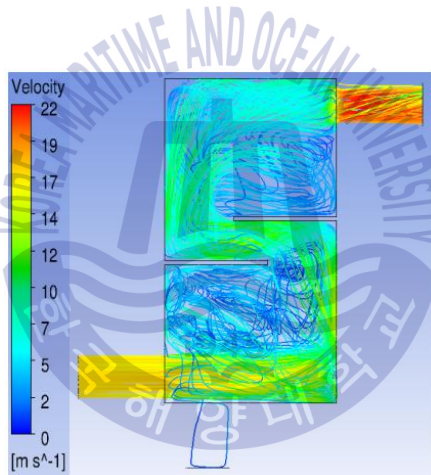


Fig. 87 Streamline of six horizontal nozzles at flow rate 160 [Nm^3/h]

Fig. 84–Fig. 87 showed that the velocity of gas increases from the inlet to the outlet. The inlet velocity at $70Nm^3/h$ was about 7m/s, the outlet velocity at $70Nm^3/h$ was about 8m/s. The inlet and outlet velocities at $100Nm^3/h$ were 11m/s and 13m/s, respectively. At a flow rate of $130Nm^3/h$, the inlet velocity was 14m/s, and the outlet velocity was 16m/s. At a flow rate of $160Nm^3/h$, the inlet and outlet velocities were 17m/s and 20m/s, respectively.

Fig. 88–Fig. 91 showed the inlet pressure was about 25Pa at $70Nm^3/h$, and the outlet pressure was about 0Pa. At a flow rate of $100Nm^3/h$, the inlet pressure was about 58Pa, and the outlet pressure was about 0Pa. At a flow rate of $130Nm^3/h$, the inlet pressure was 97Pa, and the outlet pressure was about 1Pa. At a flow rate of $160Nm^3/h$, the inlet pressure was 147Pa, and the outlet pressure was about 1Pa. Pressure decreased from the inlet to the outlet. Pressure was very high at the corners of baffles and the lower right corner.

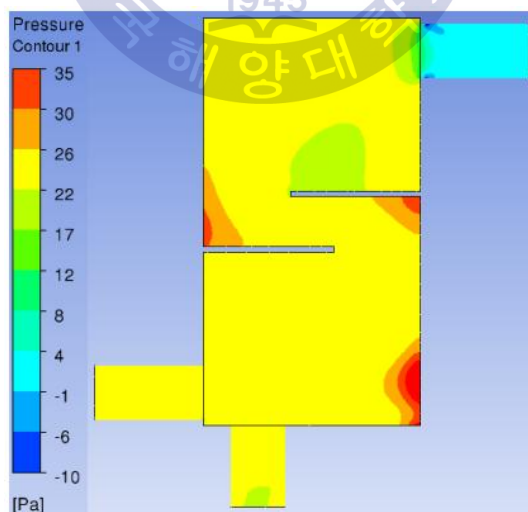


Fig. 88 Pressure contour of six horizontal nozzles at flow rate 70 [Nm^3/h]

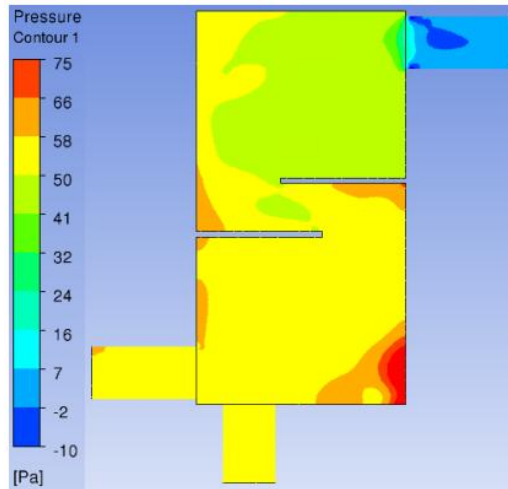


Fig. 89 Pressure contour of six horizontal nozzles at flow rate 100 [Nm^3/h]

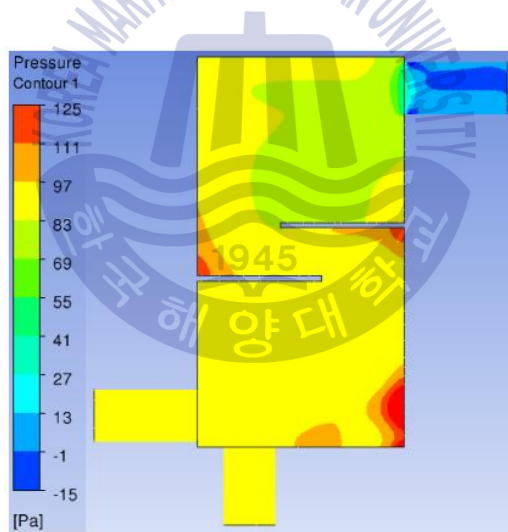


Fig. 90 Pressure contour of six horizontal nozzles at flow rate 130 [Nm^3/h]

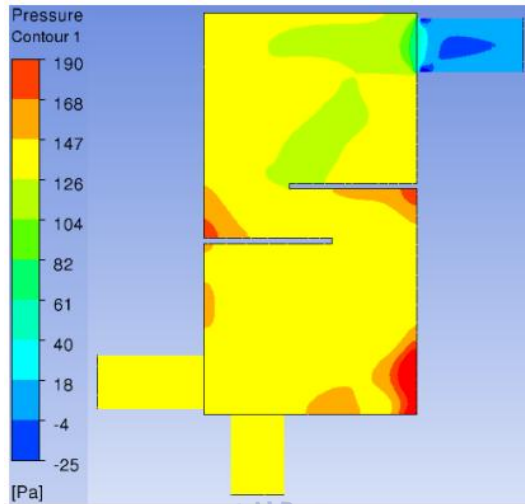


Fig. 91 Pressure contour of six horizontal nozzles at flow rate 160 [Nm^3/h]

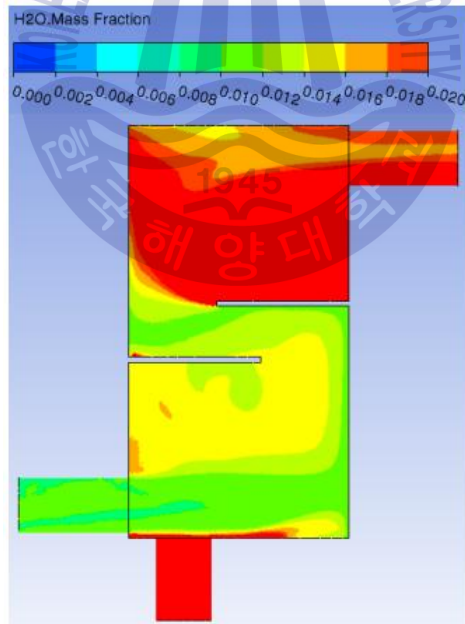


Fig. 92 Vapor contour of six horizontal nozzles at flow rate 70 [Nm^3/h]

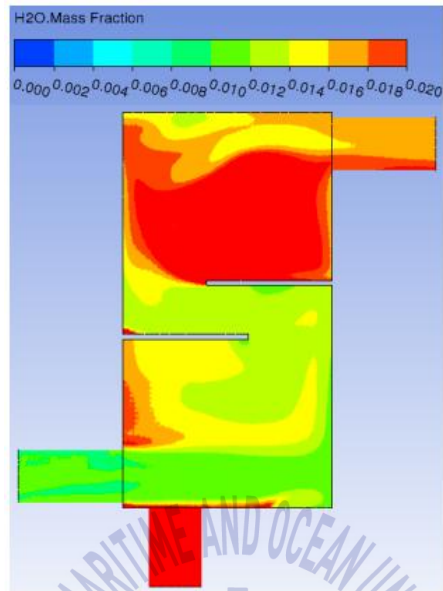


Fig. 93 Vapor contour of six horizontal nozzles at flow rate 100 [Nm^3/h]



Fig 94 Vapor contour of six horizontal nozzles at flow rate 130 [Nm^3/h]

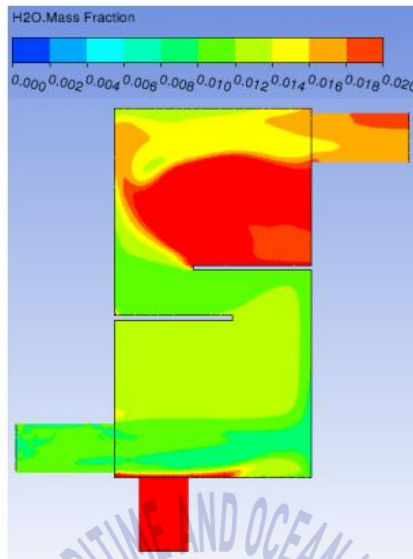


Fig. 95 Vapor contour of six horizontal nozzles at flow rate 160 [Nm^3/h]

Fig. 92–Fig. 95 showed the vapor distribution in scrubber with six horizontal nozzles. The inlet vapor under four different flow rates were all 1%. The outlet vapor at $70Nm^3/h$ was 1.9%, and was 1.8% at a flow rate of $100Nm^3/h$. The outlet vapor at $130Nm^3/h$ and $160Nm^3/h$ was 1.6% and 1.7%, respectively. The upper chambers of scrubbers were full of vapor, and the lower chambers had low level.

Chapter 4 Conclusion

The thesis based on D4AK-C diesel engine and investigated two types of scrubber for marine engines. Both volumes of scrubbers are in 60L. In the first research, it took single phase flow and discussed the influence of baffle lengths and numbers of a horizontal scrubber and a vertical scrubber on washing effect and power efficiency. The second research was conducted in two-phase flow to discuss the influence of nozzles locations and numbers on a horizontal scrubber for small marine engines.

In the case for discussing the influence of baffle length and number, it can concluded that:

For a horizontal scrubber with volume of 60L, length of 400mm, width of 200mm and height of 750mm, the optimal scheme was baffle length 240mm and 2 baffles. This structure made the pressure drop of scrubber smaller, which meant higher energy utilization. Also with higher streamline values, making the washing effect better.

For a vertical scrubber with volume of 60L, length of 1000mm, width of 300mm and height of 200mm, the optimal scheme was baffle length 210mm and 2 baffles. This structure made the pressure drop smaller and streamline values higher, which made the higher energy utilization and better washing effect.

In the case for discussing the influence of nozzle location and number, it can concluded that:

There was no big difference of pressure drop in each case, which indicated that scrubber with horizontal nozzles and vertical nozzles had the same power utilization. The vapor distributions in the scrubbers with horizontal nozzles were more uniform than those in the scrubbers with vertical nozzles. The

length of streamline in the scrubbers with horizontal nozzles were longer than that in the scrubbers with vertical nozzles. The pressure drop remained the same value at each flow rate approximately. There was no link with pressure drop and number of nozzles. With the increase of nozzle numbers, the length of streamline decreased until 4 nozzles, and then increased until 6 nozzles, and decreased from 6 to 8 nozzles finally. The scrubber with 6 horizontal nozzles has the longest length of streamline, which had the best washing effect.



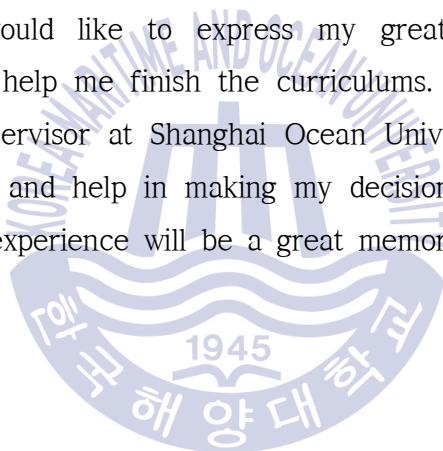
Acknowledgement

This thesis was completed in the Internal Combustion Engine Laboratory, Division of Mechanical Engineering, Korea Maritime and Ocean University (KMOU). The supervisor is Prof. Kweon Ha Park. In addition, Beom Seok Jang, Sang Min Lee and Kwun Son also provide a great help to the completion of the thesis.

First of all, I would like to express my sincere thanks to Prof. Park for accepting me to study for a master's degree in the Internal Combustion Engine laboratory. I am very grateful to Prof. Park for the help he has given me in my research and campus life during my study at Korea Maritime and Ocean University. Before I arrived in Busan, I had no contact with ANSYS and relevant software. Prof. Park instructed me directly, and help me learn how to use ANSYS-CFX soon. At the same time, Prof. Park gave me constructive advices in writing journal papers and master thesis so that I could finish my thesis smoothly. His theoretical and practical knowledge in the field of exhaust gas scrubber attracted me deeply from the bottom of my heart, and thanks to my classmates in the Internal Combustion Engine Laboratory, Beom Seok Jang, Sang Min Lee and Kwun Son, for their help. Dr. Kwun Son taught me how to use ANSYSN from the begining. Beom Seok Jang and Sang Min Lee gave me many precious suggestions when I was writing a journal paper. I want to give my thanks to the above students, when I first came to Korea Maritime and Ocean University, they helped me adapt to the life here quickly, and integrated into the laboratory. Their enthusiasm and friendliness made me feel warmth in a foreign country.

Secondly, I would like to express my sincere gratitude to my mother school Shanghai Ocean University (SHOU) for the opportunity to study abroad. It is an great honor to participate in the Double Degree Program (DDP) of Asian

Campus organized by Shanghai Ocean University and Korea Maritime and Ocean University. Thank you very much to KMOU for accepting me as a master's degree student. Through this project, I not only learned more knowledge, but also learned different customs, and I also made a deep friendship with many Korean friends. I am also highly indebted to Xu Wei, associate dean of graduate school of Shanghai Ocean University, and the faculty of graduate school for their efforts in graduation and planning for the students of Shanghai Ocean University as me who are participating in DDP between SHOU and KMOU. At the same time, I would like to thank Prof. Cheol Huh and secretary Minhwa Jeong for my great help in studying and living in KMOU. I would like to express my great appreciation to their unremitting efforts to help me finish the curriculums. Finally, I would like to thank my Chinese supervisor at Shanghai Ocean University, Prof. Yongcheng Liang, for his support and help in making my decision to go abroad. Thanks again to KMOU. This experience will be a great memory in my whole life.



References

- [1] K. Fagerholt, N. T. Gausel, J. G. Ralclce, and H. N. Psaraftis, “Maritime routing and speed optimization with emission control areas” *Transportation Research Part C*, vol. 52, pp. 57-73, 2015.
- [2] K. Cullinane, and R. Bergqvist, “Emission control areas and their impact on maritime transport” *Transportation Research Part D*, vol. 28, pp. 1-5, 2014.
- [3] O. Chiavola, F. Palmieri, and E. Recco, “Turbocharger speed estimation via vibration measurements for combustion sensing,” *Energy Procedia*, vol. 126, pp. 842-849, 2017.
- [4] A. Romagnoli, A. Manivannan, S. Rajoo, M. S. Chiong, A. Feneley, A. Pesiridis, and R. F. Martinez-Botas, “A review of heat transfer in turbochargers,” *Renewable and Sustainable Energy Reviews*, vol. 79, pp. 1442-1460, 2017.
- [5] A. Grönman, P. Sallinen, J. Honkatukia, J. Backman, and A. Uusitalo, “Design and experiments of two-stage intercooled electrically assisted turbocharger,” vol. 111, pp. 115-124, 2016.
- [6] T. Kuroki, H. Fujishima, K. Otsuka, T. Ito, M. Okubo, T. Yamamoto, and K. Yoshida, “Continuous operation of commercial-scale plasma-chemical after treatment system of smoke tube boiler emission with oxidation reduction potential and pH control,” *Thin Solid Film*, vol. 516, no. 19, pp. 6704-6709, 2008.
- [7] F. Kyriakidis, K. Sørensen, S. Singh, and T. Condra, “Modeling and optimization of integrated exhaust gas recirculation and multi-stage waste heat recovery in marine engines,” *Energy Conversion and Management*, vol. 151,

pp. 286–295, 2017.

[8] Q. Ding, X. F. Tang, and Z. G. Yang, “Failure analysis on abnormal corrosion of economizer tubes in a waste heat boiler,” *Engineering Failure Analysis*, vol. 73, pp. 129–138, 2017.

[9] I. Cornejo, P. Nikrityuk, and R. E. Hayes, “Multiscale RANS-based modeling of the turbulence decay inside of an automotive catalytic converter,” *Chemical Engineering Science*, vol. 175, pp. 377–386, 2018.

[10] M. Bal and B. C. Meikap, “Prediction of hydrodynamic characteristics of a venturi scrubber by using CFD simulation,” *South African Journal of Chemical Engineering*, vol. 24, pp. 222–231, 2017.

[11] R. W. K. Allen and A. van Santen, “Designing for pressure drop in Venturi scrubbers: the importance of dry pressure drop,” *The Chemical Engineering Journal and the Biochemical Engineering Journal*, vol. 61, no. 3, pp. 203–211, 1996.

[12] Z. Luan, X. Liu, M. Zheng, and L. Zhu, “Numerical Simulation of Square Section Venturi Scrubber with Horizontal Spray,” *Procedia Computer Science*, vol. 107, pp. 117–121, 2017.

[13] P. Goel, A. Moharana, and A. K. Nayak, “Measurement of scrubbing behavior of simulated radionuclide in a submerged venturi scrubber,” *Nuclear Engineering and Design*, vol. 327, pp. 92–99, 2018.

[14] X. Zhang, H. Li, L. Zheng, Z. Chen, and C. Qin, “Combustion characteristics of porous media burners under various back pressures: An experimental study,” *Natural Gas Industry B*, vol. 4, no. 4, pp. 264–269, 2017.

[15] H. Sapra, M. Godjevac, K. Visser, D. Stapersma, and C. Dijkstra, “Experimental and simulation-based investigations of marine diesel engine

performance against static back pressure,” *Applied Energy*, vol. 204, pp. 78–92, 2017.

[16] S. M. Lee and K. H. Park, “Study of inner structure of in-line scrubbers,” *Journal of the Korean Society of Marine Engineering*, vol. 42, no. 1, pp. 1–9, 2018 (in Korean).

[17] K. Son, J. Y. Lee, and K. H. Park, “The effect of spray flow rate, aspect ratio, and filling rate of wet scrubber on smoke reduction,” *Journal of the Korean Society of Marine Engineering*, vol. 39, no. 3, pp. 217–222, 2015 (in Korean).

[18] I. Animah, A. Addy-Lamptey, F. Korsah, and J.S. Sackey, “Compliance with MARPOL Annex VI regulation 14 by ships in the Gulf of Guinea sub-region: Issues, challenges and opportunities,” *Transportation Research PartD: Transport and Environment*, vol. 62, pp. 441–455, 2018.

[19] O. Schinas, and Ch.N. Stefanakos, “Selecting technologies towards compliance with MARPOL Annex VI: The perspective of operators,” *Transportation Research Part D: Transport and Environment*, vol. 28, pp. 28–40, 2014.

[20] G.A. Moncayo, “Testing the boundaries between the Basel and MARPOL regimes: are they complementary or mutually exclusive?” *Transportation Research Procedia*, vol. 25, pp. 233–250, 2017.

[21] X. Sun, X. Liang, G. Shu, J. lin, H. Wei, and P. Zhou, “Development of a surrogate fuel mechanism for application in two-stroke marine diesel engine,” *Energy*, vol. 153, pp. 56–64, 2018.

[22] B.-Y. Yoo, “Economic assessment of liquefied natural gas (LNG) as a marine fuel for CO₂ carriers compared to marine gas oil (MGO),” *Energy*, vol. 121, pp. 772–780, 2017.

- [23] G. Belgiorno, G. Di Blasio, and C. Beatrice, "Parametric study and optimization of the main engine calibration parameters and compression ratio of a methane-diesel dual fuel engine," *Fuel*, vol. 222, pp. 821-840, 2018.
- [24] L.M. Abadie, N. Goicoechea, and I. Galarraga, "Adapting the shipping sector to stricter emissions regulations: Fuel switching or installing a scrubber?" *Transportation Research Part D: Transport and Environment*, vol. 57, pp. 237-250, 2017.
- [25] L. Jiang, J. Kronbak, and L.P. Christensen, "The costs and benefits of sulphur reduction measures: Sulphur scrubbers versus marine gas oil," *Transportation Research Part D: Transport and Environment*, vol. 28, pp. 19-27, 2014.
- [26] I. Panasiuk, and L. Turkina, "The evaluation of investments efficiency of SO_x scrubber installation," *Transportation Research Part D: Transport and Environment*, vol. 40, pp. 87-96, 2015.
- [27] Z. Chen, H. Wang, J. Zhuo, and C. You, "Experimental and numerical study on effects of deflectors on flow field distribution and desulfurization efficiency in spray towers," *Fuel Processing Technology*, vol. 162, pp. 1-12, 2017.
- [28] Sh. Darake, M.S. Hatamipour, A. Rahimi, and P. Hamzeloui, "SO₂ removal by sea water in a spray tower: Experimental study and mathematical modeling," *Chemical Engineering Research and Design*, vol. 109, pp. 180-189, 2016.
- [29] X.-J. Tang, T. Li, H. Yu, and Y.-M. Zhu, "Prediction model for desulphurization efficiency of onboard magnesium-base seawater scrubber," *Ocean Engineering*, vol. 76, pp. 98-104, 2014.
- [30] C.-C. Tseng, and C.-J. Li, "Eulerian-Eulerian numerical simulation for a flue gas desulfurization tower with perforated sieve trays," *International Journal*

of Heat and Mass Transfer, vol. 116, pp. 329–345, 2018.

[31] I. Boscarato, N. Hickey, J. Kaspar, M.V. Prati, and A. Mariani, “Green shipping: Marine engine pollution abatement using a combined catalyst/seawater scrubber system. 1. Effect of catalyst,” *Journal of Catalysis*, vol. 328, pp. 248–257, 2015.

[32] D. Flagiello, A. Erto, A. Lancia, and F. Di Natale, “Experimental and modelling analysis of seawater scrubbers for sulphur dioxide removal from flue-gas,” *Fuel*, vol. 214, pp. 254–263, 2014.

